Copy 5
RM L52J22

NACA

RESEARCH MEMORANDUM

A SMALL-SCALE INVESTIGATION OF THE EFFECT OF SPANWISE AND CHORDWISE POSITIONING OF AN OGIVE-CYLINDER UNDERWING NACELLE ON THE HIGH-SPEED AERODYNAMIC CHARACTERISTICS OF A 45° SWEPTBACK TAPERED-IN-THICKNESS WING OF ASPECT RATIO 6

By H. Norman Silvers and Thomas J. King, Jr.

Langley Aeronautical Laboratory
Langley Field, Va.

NATIONAL ADVISORY COMMITTEE
FOR AERONAUTICS

WASHINGTON

December 18, 1952

NATIONAL ADVISORY COMMITTEE FOR AERONAUTICS

RESEARCH MEMORANDUM

A SMALL-SCALE INVESTIGATION OF THE EFFECT OF SPANWISE AND CHORDWISE POSITIONING OF AN OGIVE-CYLINDER UNDERWING NACELLE ON THE HIGH-SPEED AERODYNAMIC CHARACTERISTICS OF A 45° SWEPTBACK TAPERED-IN-THICKNESS WING OF ASPECT RATIO 6

By H. Norman Silvers and Thomas J. King, Jr.

SUMMARY

A nacelle was investigated in three chordwise locations at each of four spanwise locations in an underwing position on a small-size semispan model of a wing sweptback 45° and tapering in thickness from 9 percent at the root to 3 percent at the tip. The investigation was made to determine the effect of the nacelle in a wide range of locations on the high-speed aerodynamic characteristics of a sweptback wing without a fuselage.

The results indicated, in general, that reductions in nacelle-drag coefficient (including interference drag) come from rearward chordwise movement of the nacelle through the range of chordwise and spanwise positions investigated, except at the extreme tip location where, for the higher lift coefficients, minimum nacelle drag was obtained for intermediate chordwise locations. The nacelle-drag coefficients of the nacelles at both the extreme inboard and the tip locations were shown to be critically dependent upon model lift coefficient. The highest maximum lift-drag ratios of the model with nacelles were obtained with the nacelle located at the most rearward chordwise positions. The most significant over-all effects of nacelle positioning on the lift- and pitching-moment-curve slopes were shown for chordwise positioning at inboard spanwise locations where a change from forward to rearward nacelle locations produced a stabilizing change in the aerodynamic-center location from 12- to 25-percent mean aerodynamic chord over the Mach number range investigated. At high lift coefficients the destabilizing pitch-up of the wing was minimized at all nacelle chordwise locations for middle-span locations of the nacelle.

INTRODUCTION

The National Advisory Committee for Aeronautics is conducting a program of research on nacelles and external stores in order to provide information for the design of installations suitable for use on airplanes at transonic speeds. The investigations of this program are concerned with an over-all evaluation of the effects of body positioning and shape on the aerodynamic characteristics of models with straight and sweptback wings.

The present paper is the first of a series of papers reporting the results of investigations made in the Langley high-speed 7- by 10-foot tunnel as part of the general program. The results presented in this paper show the effect of spanwise and chordwise positioning of an underwing, ogive-cylinder nacelle on a 45° sweptback wing without a fuselage. Results showing the effects of variations in body shape and vertical positioning and the effect of a fuselage on a vertically symmetric nacelle in several spanwise locations will be presented in subsequent papers.

In the investigations of nacelles made in the Langley high-speed 7- by 10-foot tunnel as well as those made earlier by the Pilotless Aircraft Research Division (refs. 1 to 5), a wing has been used having a sweepback angle of 45°, an aspect ratio of 6, a taper ratio of 0.6, and NACA 65A-series airfoil sections. The wing used in the Langley high-speed 7- by 10-foot-tunnel investigations, however, was tapered in thickness from 9 percent at the root to 3 percent at the tip, whereas the wings of the flight models were 9 percent thick from root to tip.

The results obtained in this series of investigations are considered to be exploratory in nature. By covering a broad range of nacelle positioning variables, these investigations are intended to show nacelle positions of particular research interest in order that later investigations may be directed toward developing a better understanding of the flow characteristics over the nacelle installations. These papers are also intended to supplement the zero-lift drag results obtained in earlier flight investigations (refs. 1 to 5) by covering a range of lift coefficients extending from about 0 to about 0.5 and also by showing the effects of nacelle geometry and positioning on wing lift, pitching moment, and bending moment.

SYMBOLS

C_L lift coefficient, $\frac{\text{Twice semispan lift}}{qS_w}$

C_D drag coefficient, $\frac{\text{Twice semispan drag}}{qS_w}$

C_{D_n} nacelle-drag coefficient, $\left(C_{D_{\text{model+nacelle}}} - C_{D_{\text{model}}}\right)\frac{S_w}{2S_n}$

C_m pitching-moment coefficient referred to $0.25\bar{c}$ of wing, $\frac{\text{Twice semispan pitching moment}}{qS_w\bar{c}}$

C_B bending-moment coefficient, $\frac{\text{Twice root bending moment}}{qS_w\frac{b}{2}}$

q free-stream dynamic pressure, $\frac{1}{2}\rho V^2$, lb/sq ft

S_w twice wing area of semispan model, 0.125 sq ft

S_n maximum frontal area of nacelle, 0.00119 sq ft

$\bar{c}$ mean aerodynamic chord of wing, $\frac{2}{S_w}\int_0^{b/2} c^2 dy$ (using theoretical tip), 0.147 ft

c local wing chord parallel to free stream, ft

b twice span of semispan model, 0.866 ft

d nacelle diameter, ft

x longitudinal distance from wing leading edge at nacelle spanwise location to nose of nacelle; negative when nose of nacelle is forward of wing leading edge, ft

y lateral distance from plane of symmetry to center line of nacelle, ft

l nacelle length, 0.364 ft

V effective free-stream air velocity, ft/sec

M effective Mach number, $\frac{2}{S_w}\int_0^{b/2} cM_a dy$

M_l local Mach number obtained from calibration made without a model in place on the reflection-plane plate

M_a average chordwise Mach number

ρ mass density of air, slugs/cu ft

α angle of attack, deg

y_{cp} lateral center of pressure referred to wing semispan, $\partial C_B/\partial C_L$

$C_{L_\alpha} = \left(\frac{\partial C_L}{\partial \alpha}\right)_M$

$C_{m_{C_L}} = \left(\frac{\partial C_m}{\partial C_L}\right)_M$

APPARATUS AND MODELS

This investigation was conducted in the Langley high-speed 7- by 10-foot tunnel and utilized a small semispan model mounted on a reflection-plane plate, which was located 3 inches from the tunnel wall in order to bypass the wall boundary layer (fig. 1). The semispan model was attached to a strain-gage balance by a projection of the root chord which passed through the reflection-plane plate. To prevent fouling of the model, a clearance of approximately 1/32 inch was maintained between the root chord and the reflection-plane plate. The strain-gage balance was attached to the outside of the tunnel and, to minimize leakage of air into the flow field of the model, the balance was housed in a sealed container.

The semispan wing model was constructed of steel and had an angle of sweepback of 45° referred to the quarter-chord line, an aspect ratio of 6, a taper ratio of 0.6, and NACA 65A-series airfoil sections parallel to the air stream that tapered in thickness from 9 percent at the root to 3 percent at the tip.

The nacelle used in this investigation was similar, in general, to the nacelles used in references 1 to 5, in that all nacelles were formed from ogival nose and tail sections and a cylindrical midsection. The tail section of the nacelle of this investigation terminated in a point (fig. 2), whereas the tail sections of the nacelles of references 1 to 5

had a blunt end; that is, the extreme rearward portions of the ogival tail sections were removed. The fineness ratios of the nacelles, based on the actual body lengths tested, were 9.34 for the nacelle of this investigation and 9.66 for the nacelles of references 1 to 5.

The nacelle of this investigation was somewhat larger compared to the wing than the nacelles of references 1 to 5. The size of the nacelle used herein was established from existing jet-engine specifications and, based on an assumed model scale of 0.01, would result in a full-scale nacelle of approximately 47 inches in diameter. At this scale the airplane would be of the medium-bomber class. Ordinates of the nacelle are presented in table I.

In each chordwise and spanwise position the nacelle was located so that the distance between the chord plane of the wing and the nacelle center line was equal to the maximum radius of the nacelle. Three chordwise locations referred to herein as rearward, intermediate, and forward were investigated in each of four spanwise locations. Test locations of the nacelle are shown in figure 2. The chordwise locations of the nacelle were obtained by using constant distance between nacelle nose and wing leading edge. This procedure resulted in different nondimensional locations (as shown in table of fig. 2) when referred to the local chord which varies because of the taper of the wing.

METHODS AND TESTS

The reflection-plane plate attached to the wall of the Langley high-speed 7- by 10-foot tunnel induces over its surface a region of local velocities higher than the free-stream velocities of the tunnel test section, which permits testing of small models to Mach numbers of 1.08. The variations in local Mach numbers over the reflection-plane plate are shown in figure 3 for average test Mach numbers. As indicated by these data, the Mach number gradient in the region occupied by the model decreases with decreasing tunnel speed. At a Mach number of about 0.93, the flow becomes gradient free. Effective Mach numbers, which were used as the basis of data presentation, were obtained by integration of the contours by the relationship

$$M = \frac{2}{S}\int_0^{b/2} cM_a \, dy$$

Lift, drag, pitching-moment, and bending-moment coefficients were obtained over an angle-of-attack range that extended from about -1.5°

[redacted]

to 9.0° at Mach numbers ranging from 0.7 to 1.08. The variation of Reynolds number with Mach number for these tests is shown in figure 4. Because of the small size of the model employed in this investigation, jet-boundary and blockage corrections were considered negligible.

In general, an indication of the accuracy of the force and moment measurement is given by any random scatter of the test points of the basic data. In determining increments of forces and moments, however, faired values of forces and moments are used, thus tending to minimize the influence of test-point scatter on the curves of summary results.

Experience with the technique of locating small reflection-plane models in a localized high-velocity field to obtain transonic speeds has indicated that absolute values of coefficients, particularly drag, sometimes do not correlate well with data obtained on larger models using other test techniques. Valid incremental effects, such as those due to model configuration, lift coefficient, or Mach number, are, however, believed to be obtained by this technique. These conclusions were reached after a correlative study (ref. 6) had been made between results obtained from bump-type test techniques and conventional techniques in which a sting support was used. Subsequent experience with nacelle and external-store testing has also shown that the trends of drag increments due to nacelle configurations, which are obtained from reflection-plane models investigated on bump-type test facilities, appear to be in qualitative agreement with those results obtained on larger-scale three-dimensional models tested in flight.

RESULTS AND DISCUSSION

The results of this investigation are presented in figures and the content is summarized as follows:

	Figure
Basic data:	
Wing alone	5
Wing with nacelle at various locations	6 to 9
Summary figures:	
Drag characteristics	9 to 13
Maximum lift-drag ratio	13 and 14
Lift-curve slope	15 and 16
Pitching-moment-curve slope	17 and 18
Lateral center of pressure	19 and 20

Lift-curve slopes presented were measured through zero lift, whereas pitching-moment-curve slopes were measured at a lift coefficient of 0.1.

Drag Characteristics

The variations in drag coefficients with Mach number for the model with and without nacelles are presented in figure 9. These results show an important effect of speed on the drag due to the nacelles in the transonic speed range. At low lift coefficients the drag due to the nacelles is, in general, considerably higher at Mach numbers above force break than at lower speeds. Such characteristics have been shown before in flight investigations made at zero lift (refs. 1 to 5).

Before a more detailed discussion of the effect of lift as well as the effect of nacelle position on nacelle-drag coefficient is undertaken, it is of interest to discuss the drag-break characteristics as shown from the total drag coefficients (fig. 9). At low lift coefficients the nacelle locations for the highest Mach numbers of initial drag divergence appear to occur for the rearward nacelle in spanwise locations from 0.46b/2 to 0.96b/2. Although somewhat lower than those for the rearward nacelle, the Mach numbers for drag divergence are also high for tip mountings (0.96b/2) of the intermediate and forward nacelles at low lift coefficients. It is of interest to note that, at the higher lift coefficients, nacelle locations for which the nacelle drag is the lowest usually have considerably lower Mach numbers for drag divergence than the nacelle locations for which the drag is higher.

The nacelle-drag coefficients, defined as the increment in drag due to the nacelles plus interference based upon nacelle maximum frontal area, are presented in figure 10 as a function of lift coefficient, in figure 11 as a function of nacelle spanwise location, and in figure 12 as a function of nacelle chordwise location. These data (figs. 10 to 12) show that the inboard and the tip locations of the nacelle are the spanwise nacelle locations subject to the largest changes in nacelle-drag coefficients due to change in lift coefficient throughout the Mach number range. It is also seen that, in general, the rearward nacelle is subject to larger changes in C_{D_n} throughout the range of spanwise locations because of changes in lift than is either the intermediate or forward nacelle location. It appears then that extreme locations of the nacelle either spanwise or chordwise (when the nacelle is rearward) result in interference effects that are critically dependent upon model lift coefficient on a model without a fuselage. It has also been shown (ref. 5) that, on a model with a fuselage, the inboard and tip locations of a nacelle produced nacelle-drag coefficients much lower than those of intermediate spanwise locations. These results, available only at zero lift, agree qualitatively with unpublished results obtained as another phase of the present investigation, which show the effect of a fuselage by comparison with the results presented herein on a wing without a fuselage.

Very little quantitative information is available to explain the large changes in interference found for some extreme locations of nacelles.

At transonic speeds, however, the development and movement of shock waves with change in Mach number and lift coefficient can have considerable effect on interference. It has been shown recently (ref. 7) that shock waves induced by a fuselage can extend beyond the wing tip with little diminution in intensity. Thus, nacelles located even at the wing tip could be affected by fuselage-induced shock conditions. It should be emphasized that, although fuselage effects appear to be an important factor in nacelle interference at transonic speeds, not enough is known about fuselage effects in this speed range to permit generalization applicable to particular designs. As a step toward developing an understanding of nacelle interference on a wing without a fuselage, it is desirable to examine the results presented herein.

Favorable interference exists at the higher lift coefficients for extreme inboard nacelle locations if the nacelle is located rearward on the wing chord, because in this location an increase in lift produces considerable reductions in nacelle-drag coefficient throughout the Mach number range investigated. A tip location of a forward nacelle is seen to give rather abrupt increases in C_{D_n} with increases in lift coefficient at lift coefficients greater than about 0.3. A rearward location of the inboard nacelle and a forward location of the tip nacelle are of particular design interest because on a sweptback wing these locations result in a minimum longitudinal displacement of weight away from the center of gravity of an airplane. For this reason intermediate nacelles at midspan locations are also widely used. The nacelle-drag coefficients of the intermediate nacelle at 0.46b/2, although varying little with lift coefficient at Mach numbers of 0.90 and 1.08, are seen to be somewhat higher than those of the rearward nacelle in the inboard location. It is important to note in the interest of low nacelle drag that the rearward nacelle generally gives lower C_{D_n} for all spanwise locations, except for the higher lift coefficients when located at the extreme tip as will be pointed out later.

Figure 12 is presented to show the variation of nacelle-drag coefficient with nacelle chordwise position. These results indicate that the most pronounced effect on C_{D_n} of changes in chordwise location exists for the extreme inboard nacelle location and the tip nacelle location which have been shown earlier to be critically affected by C_L. As indicated previously in this paper, a rearward location for a nacelle is a promising low-drag location except at the tip (0.96b/2) location for higher lift coefficients, where minimum nacelle-drag coefficients were obtained for the intermediate chordwise nacelle locations. Rearward nacelle locations have also been shown to be low-drag locations in another investigation using a nacelle of lower fineness ratio and different profile shape (ref. 8).

[redacted]

Lift-Drag Ratios

The variations in maximum lift-drag ratios for the models both with and without nacelles in the various test positions are presented in figure 13. It has been found convenient in obtaining a quantitative expression of the effect of the nacelles on the maximum lift-drag ratio of the model to divide the $(L/D)_{max}$ of the model with nacelles by $(L/D)_{max}$ of the model without nacelles. Presented in figure 14 are these ratios as a function of nacelle spanwise location. Discussion of the effect of nacelle position will be concerned with these ratios. It is seen that a ratio value of less than 1.0 was obtained for all conditions of this investigation; that is, the $(L/D)_{max}$ of the model with nacelle was always less than that of the model without nacelles.

As may be anticipated from the foregoing discussion of nacelle-drag coefficient, the nacelle chordwise location for the highest $(L/D)_{max}$ is the rearward location. In general, the highest maximum lift-drag ratios of the rearward nacelle are obtained at spanwise positions from $0.4b/2$ to $0.5b/2$ where they are about 91 percent of the $(L/D)_{max}$ of the model without nacelles. The $(L/D)_{max}$ obtained with the rearward nacelle is also from 8 to 13 percent (based on $(L/D)_{max}$ of the model) higher than that of the next best chordwise location.

The large variations of nacelle-drag coefficient shown previously at the higher lift coefficients for the extreme inboard and tip nacelle locations are not reflected in the maximum lift-drag ratios because the lift coefficients for $(L/D)_{max}$ are somewhat below the lift coefficients at which these variations in C_{D_n} were found.

Lift Characteristics

The variations in lift-curve slope with Mach number of the model with and without nacelles in the various positions investigated are presented in figure 15. To aid in determining the effects of nacelle position on the lift-curve slope, the incremental changes in C_{L_α} due to the nacelles have been taken and are presented in figure 16 as a function of nacelle spanwise location. These data indicate that the types of variations found in the subsonic speed range for the three nacelle chordwise positions investigated are considerably different from those shown at a supersonic Mach number of 1.08. At subsonic speeds, there is a range of spanwise locations (which varies with speed but usually lies within $0.30b/2$ to $0.70b/2$) in which the forward and

rearward nacelles have little effect on the lift-curve slope of the model. Outside of this range, some increase in C_{L_α} occurs. On the other hand, the intermediate nacelle is seen to produce a maximum increase within this spanwise range that is as much as 15 percent of C_{L_α} of the basic model. At a supersonic Mach number of 1.08, however, the intermediate nacelle is seen to produce the minimum increase in C_{L_α} in this spanwise range, whereas high C_{L_α} increments have developed for the rearward nacelle.

It is of interest to note that, in general, a tip mounting of the nacelle increased the lift-curve slope of the model except for the rearward nacelle at $M = 1.08$. This condition may be expected as it is commonly known that a tip-mounted nacelle effectively provides an end plate for the wing. The increase in effective aspect ratio coming from such a condition has in some instances materially reduced drag due to lift of the model with tip mounted nacelle over the drag due to lift of models with nacelles at more inboard locations. Drag results (fig. 10) show, however, that such a result is generally not the case in this investigation, probably because of the adverse effects of lift coefficient on the flow at wing-nacelle junctures for some of the tip configurations, a condition which might be improved by fairing of the wing-nacelle junctures.

Pitching-Moment Characteristics

The effects of nacelle positioning on the stability characteristics of the model as indicated by the increments in slopes of the pitching-moment curves are presented in figure 18, and were obtained from figure 17. The pitching-moment data from which the slopes were obtained (figs. 5 to 8) showed considerable nonlinearity for some nacelle locations and some Mach numbers at the lower lift coefficients where pitching-moment slopes are usually taken. The slopes presented were obtained at a lift coefficient of 0.1 and, because of the nonlinearities, cannot be used for analysis at other lift coefficients. Comparison of the pitching-moment curves for the model with the nacelle in various positions with those of the model without nacelle show that the major nonlinearities, at low lift coefficients, occurred only for the model with nacelle. It is not known whether this apparent effect of the nacelle on the stability characteristics would be encountered at higher Reynolds numbers or not. In spite of the nonlinearities, it appears desirable to indicate several general observations about the effect of nacelle positions on the stability of the model at $C_L = 0.1$.

Markedly different variations in the increments in pitching-moment-curve slope (fig. 18) are seen to exist at subsonic and supersonic speeds.

The more important effects of speed on $\Delta C_{m_{C_L}}$ are found for the forward and the rearward nacelles. At subsonic Mach numbers the forward nacelle is seen to produce a decrease in stability of the model which varies little for the various spanwise positions investigated in comparison to the variations in $\Delta C_{m_{C_L}}$ shown at $M = 1.08$, where a change in $\Delta C_{m_{C_L}}$ equivalent to a change in aerodynamic-center location of 22.5-percent mean aerodynamic chord occurs. The rearward nacelle, however, shows little effect of spanwise location on the increment in pitching-moment-curve slope at $M = 1.08$ but rather abrupt and sizable changes at subsonic speed. In this speed range the most serious changes in $\Delta C_{m_{C_L}}$ for the rearward nacelle is seen to occur over a spanwise range from about 0.50 to 0.70b/2 where the rearward nacelle changes from the chordwise location contributing the largest instability to the chordwise location contributing the largest stability. Because of these characteristics an over-all increase in stability occurs as a result of movement of the nacelle from a forward to a rearward location in inboard spanwise positions that is equivalent to a 12- to 25-percent change in the mean-aerodynamic-center location.

In addition to the static longitudinal stability as indicated by $\Delta C_{m_{C_L}}$ taken at a lift coefficient of 0.1, it is of interest to examine the effect of nacelle location on the stability characteristics at high lift coefficients. The results, figure 5, show that, in this lift range, the wing without nacelle encounters destabilizing pitch-up at lift coefficients somewhat higher than about 0.3 throughout the Mach number range. The results obtained with the nacelle in place indicate that several locations of the nacelle are effective in minimizing pitch-up of the wing at high C_L. It appears that the maximum benefit is obtained for middle-span locations of the nacelle. With the rearward nacelle, pitch-up of the wing is reduced with the nacelle at 0.70b/2, whereas with a forward nacelle, it is reduced with the nacelle at 0.46b/2. It is interesting to note that, with the intermediate nacelle, pitch-up is minimized at both 0.46b/2 and 0.70b/2.

Lateral Center of Pressure

The increments in lateral center-of-pressure locations obtained from figure 19 are presented in figure 20. An examination of these results does not reveal such obvious Mach number effects as were found in the increments of lift-curve slope or pitching-moment-curve slope in passing from subsonic to supersonic speeds. In general, outboard movement of the nacelle from a location of 0.20b/2 produces an inboard movement of the lateral center of pressure from that of the model without nacelles until, at some spanwise location, a maximum inboard location

of y_{cp} is obtained after which further outboard movement of the nacelle results in outboard movement of y_{cp}. The wing-tip nacelle seems to produce an additional loading of the wing tip so that an over-all outboard movement of y_{cp} results. The largest change in Δy_{cp} found for the three chordwise locations investigated was shown for the rearward nacelle at the wing tip at a Mach number of 1.08 where about a 5-percent outboard movement of the lateral center of pressure occurred as the nacelle was moved from 0.7lb/2 to 0.96b/2. The principal effects of increasing Mach number appear to be an outboard displacement of the spanwise location for maximum inboard location of y_{cp} and a more outboard location of y_{cp} for the nacelle at the wing tip. The over-all changes in lateral center of pressure due to the nacelles in various spanwise and chordwise locations were found to be within about 3 percent semispan at subsonic speeds and 6 percent semispan at supersonic speeds.

CONCLUSIONS

The results of an investigation of an underwing ogive-cylinder nacelle in three chordwise positions at each of four spanwise locations on the aerodynamic characteristics of a 45° sweptback, tapered-in-thickness wing at small Reynolds numbers indicate the following conclusions:

1. In general, reductions in nacelle-drag coefficient (including interference drag) result from rearward chordwise movement of the nacelle through the spanwise range investigated, except at the extreme tip location at the higher lift coefficients where minimum nacelle drag was obtained for more intermediate chordwise locations.

2. Both the extreme inboard and tip locations of the nacelle showed a critical dependence of nacelle-drag coefficient on lift coefficient throughout the speed range investigated. For the inboard location the largest changes in nacelle-drag coefficient due to lift coefficient were shown for the rearward nacelle, where appreciable reductions in nacelle drag came with increase in lift; for the tip location, the largest changes in nacelle drag occurred for the forward nacelle, where increase in lift coefficient produced significant increases in nacelle drag.

3. The highest maximum lift-drag ratios of the model with nacelles were obtained with the nacelle in the rearward location. With this chordwise location, the highest maximum lift-drag ratios were obtained at near midsemispan nacelle locations where the maximum lift-drag ratio of the model with nacelle was of the order of 91 percent of that of the model without nacelle.

4. Characteristically different variations in the increments in slopes of the lift- and pitching-moment curves due to the various nacelle positions were obtained at subsonic and supersonic Mach numbers. The most significant effects of changes in nacelle spanwise and chordwise positions on the increments in lift- and pitching-moment-curve slopes were shown in the pitching-moment-curve slopes where changes in nacelle chordwise position from forward to rearward in inboard spanwise locations produced from 12- to 25-percent stabilizing changes in the aerodynamic-center locations referred to the mean aerodynamic chord.

5. Nacelle spanwise location had a significant effect on the stability characteristics of the wing at high lift coefficients. Midsemi-span locations of the nacelle appeared to minimize the destabilizing pitch-up tendency of the wing at high lift coefficients for all chordwise positions of the nacelle.

Langley Aeronautical Laboratory,
National Advisory Committee for Aeronautics,
Langley Field, Va.

REFERENCES

1. Pepper, William B., Jr., and Hoffman, Sherwood: Transonic Flight Tests To Compare the Zero-Lift Drag of Underslung and Symmetrical Nacelles Varied Chordwise at 40 Percent Semispan of a 45° Sweptback, Tapered Wing. NACA RM L50G17a, 1950.

2. Pepper, William B., Jr., and Hoffman, Sherwood: Comparison of Zero-Lift Drags Determined by Flight Tests at Transonic Speeds of Symmetrically Mounted Nacelles in Various Spanwise Positions on a 45° Sweptback Wing and Body Combination. NACA RM L51D06, 1951.

3. Hoffman, Sherwood: Comparison of Zero-Lift Drag Determined by Flight Tests at Transonic Speeds of Pylon, Underslung, and Symmetrically Mounted Nacelles at 40 Percent Semispan of a 45° Sweptback Wing and Body Combination. NACA RM L51D26, 1951.

4. Hoffman, Sherwood, and Pepper, William B., Jr.: Transonic Flight Tests To Determine Zero-Lift Drag and Pressure Recovery of Nacelles Located at the Wing Tips on a 45° Sweptback Wing and Body Combination. NACA RM L51K02, 1952.

5. Hoffman, Sherwood: Transonic Flight Tests To Compare the Zero-Lift Drags of Underslung Nacelles Varied Spanwise on a 45° Sweptback Wing and Body Combination. NACA RM L52D04a, 1952.

6. Donlan, Charles J., Meyers, Boyd C., II, and Mattson, Axel T.: A Comparison of the Aerodynamic Characteristics at Transonic Speeds of Four Wing-Fuselage Configurations as Determined From Different Test Techniques. NACA RM L50H02, 1950.

7. Whitcomb, Richard T., and Kelly, Thomas C.: A Study of the Flow Over a 45° Sweptback Wing-Fuselage Combination at Transonic Mach Numbers. NACA RM L52D01, 1952.

8. Silvers, H. Norman, King, Thomas J., Jr., and Pasteur, Thomas B., Jr.: Investigation of the Effect of a Nacelle at Various Chordwise and Vertical Positions on the Aerodynamic Characteristics at High Subsonic Speeds of a 45° Sweptback Wing With and Without a Fuselage. NACA RM L51H16, 1951.

[redacted]

TABLE I. - NACELLE ORDINATES

[Fineness ratio 9.34]

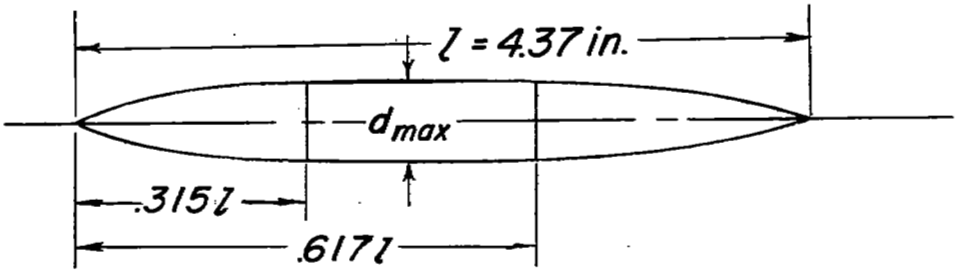

Ordinates, percent length	
Station	Radius
0.	0.
.36	.30
1.21	.73
3.04	1.44
4.87	2.09
6.71	2.65
8.26	3.07
9.15	3.29
9.69	3.44
10.84	3.70
11.99	3.94
13.14	4.12
14.29	4.20
15.44	4.44
17.74	4.70
20.04	4.92
22.34	5.08
24.64	5.20
26.94	5.30
29.24	5.34
31.54	5.36
61.70	5.36
68.69	5.20
74.95	4.76
81.22	3.94
87.48	2.76
90.60	2.11
93.75	1.42
96.89	.72
98.44	.36
100.00	0.

NACA

[redacted]

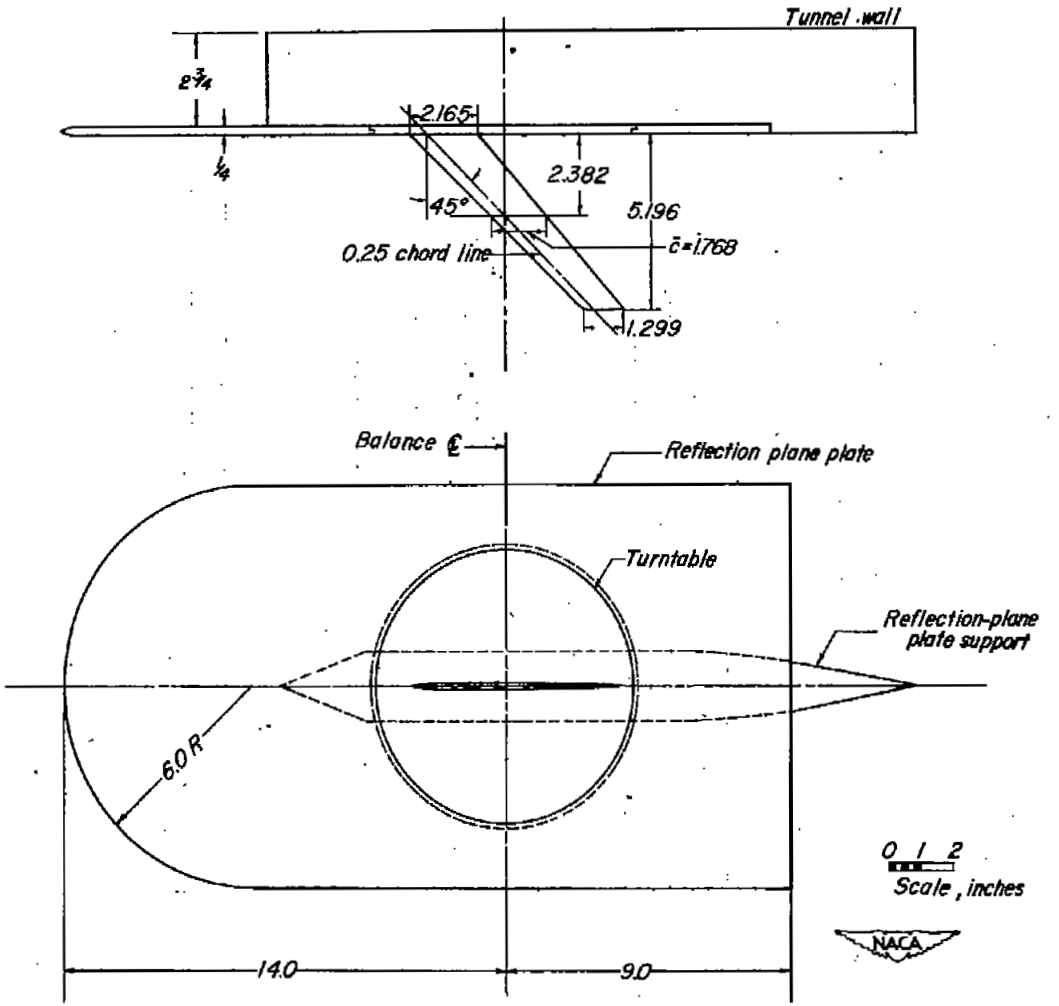

Figure 1.- Two-view drawing of the 45° sweptback semispan wing of aspect ratio 6, taper ratio 0.6, and an NACA 65A-series airfoil section tapered in thickness from 9 percent at the root to 3 percent at the tip.

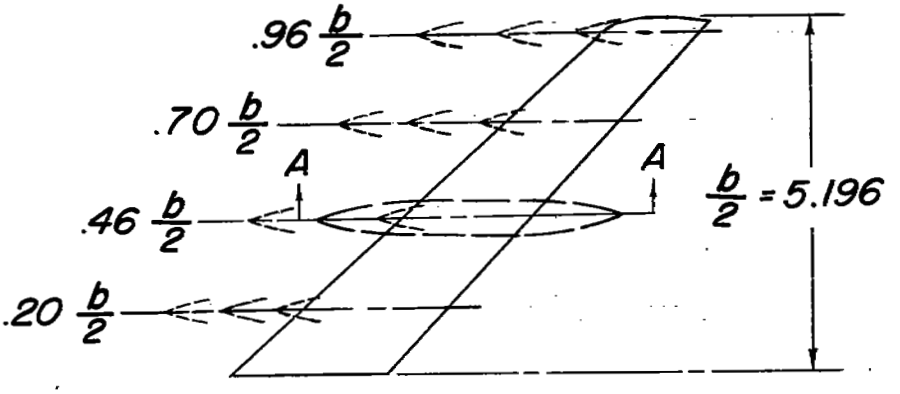

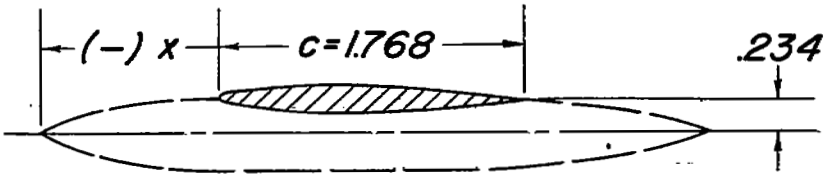

Section A-A

	Nacelle Chordwise Locations, x/c			
Chord designation \ y/(b/2)	.20	.46	.70	.96
Forward	-.946	-1.192	-1.486	-1.897
Intermediate	-.556	-.698	-.859	-1.083
Rearward	-.181	-.204	-.231	-.269

Figure 2.- Drawing showing the locations of the nacelle on the test model. All dimensions are in inches.

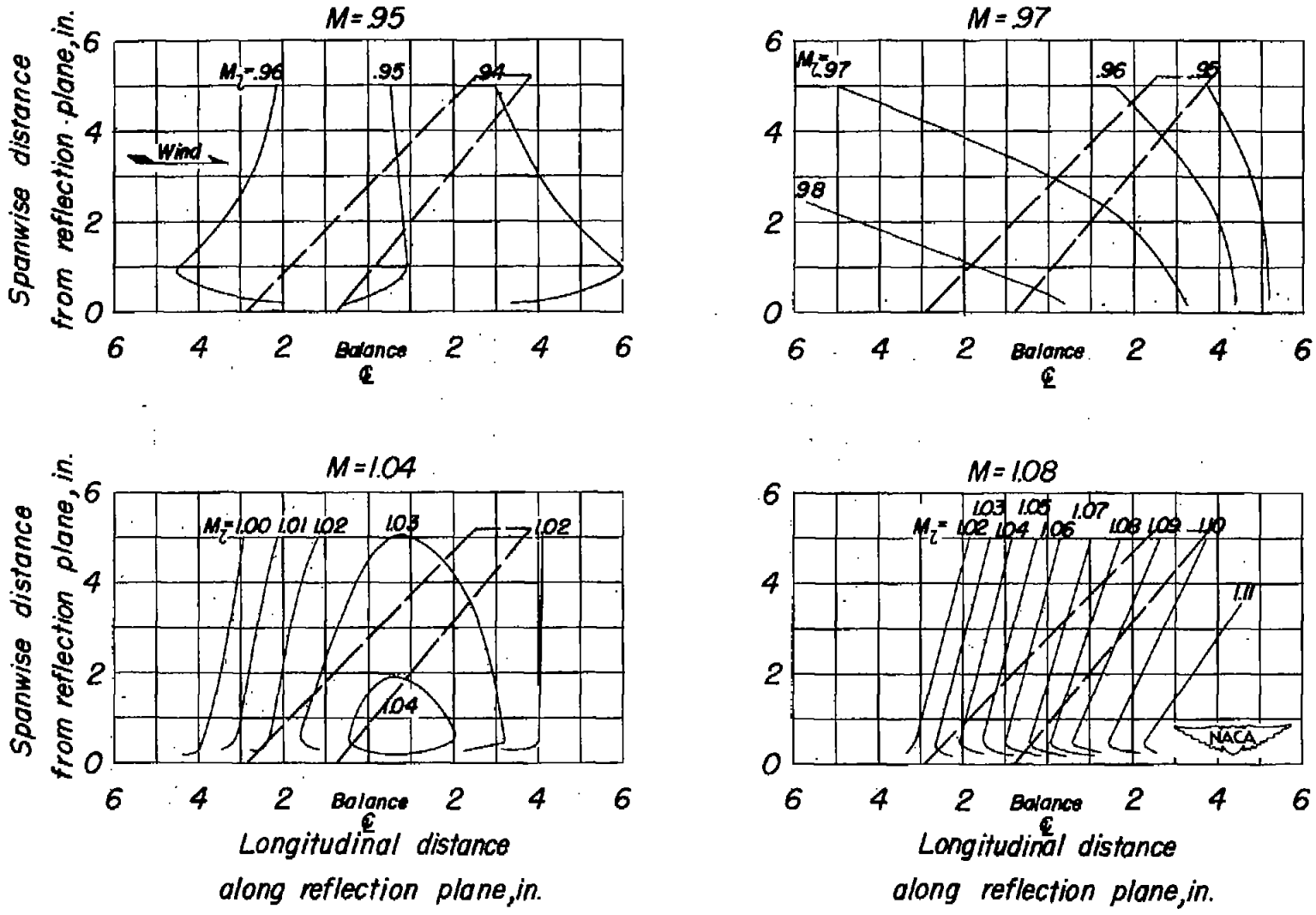

Figure 3.- Typical Mach number contours over side-wall reflection plane in region of model location.

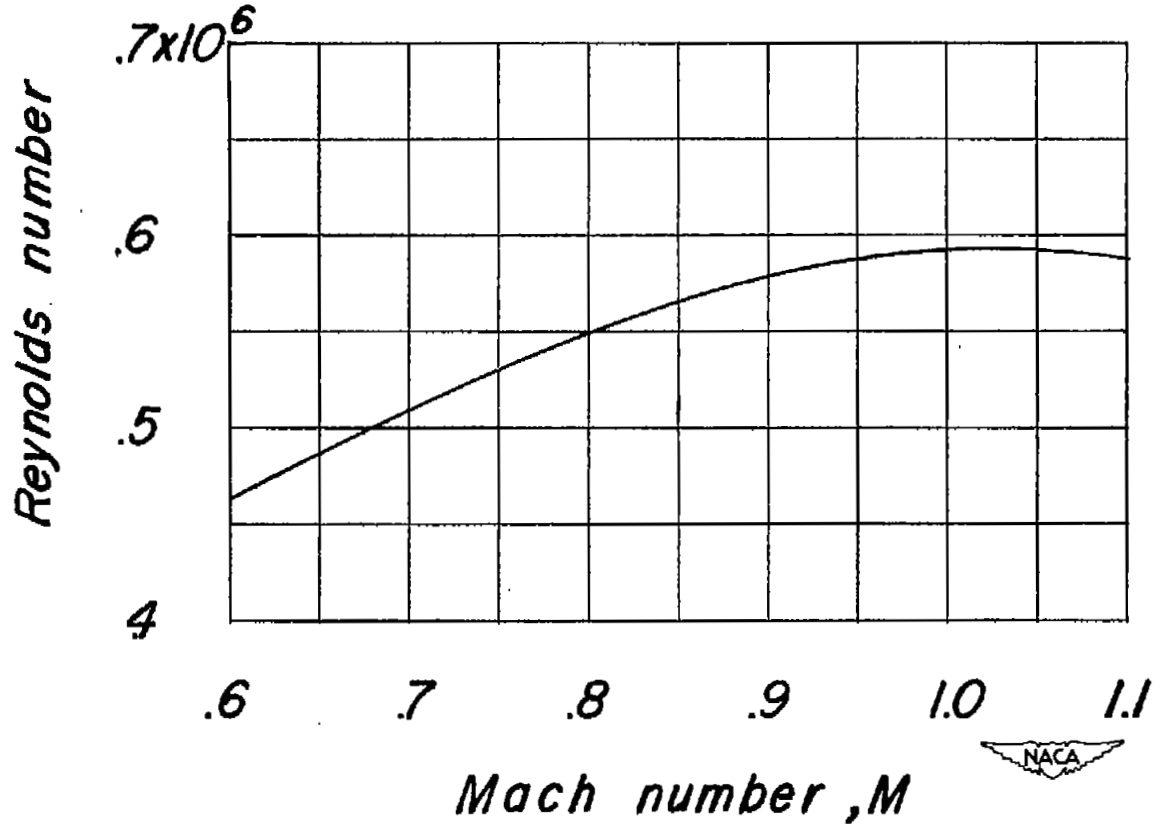

Figure 4.- Variation of Reynolds number with Mach number for the model in the Langley high-speed 7- by 10-foot tunnel.

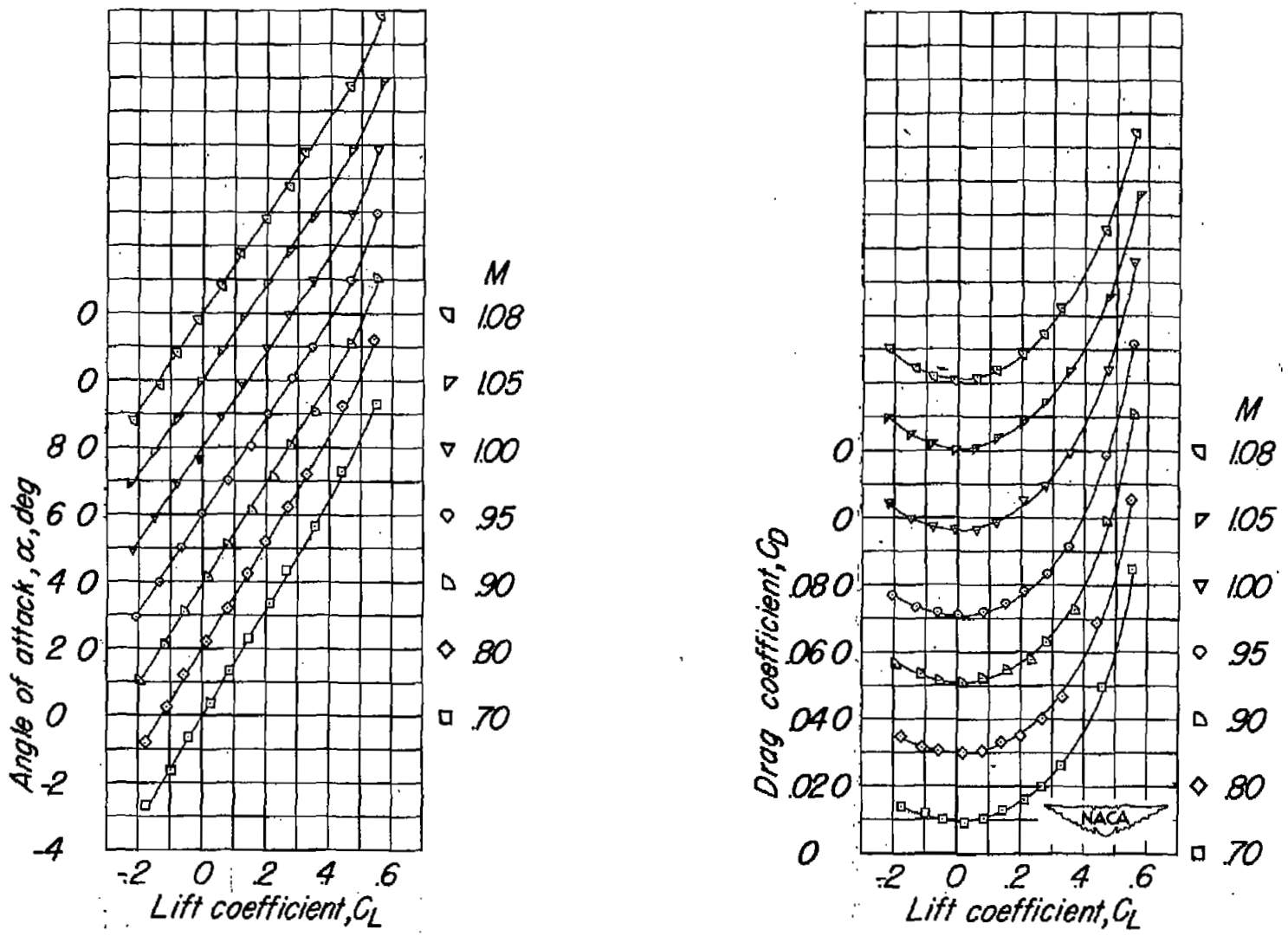

Figure 5.- Aerodynamic characteristics of the semispan wing.

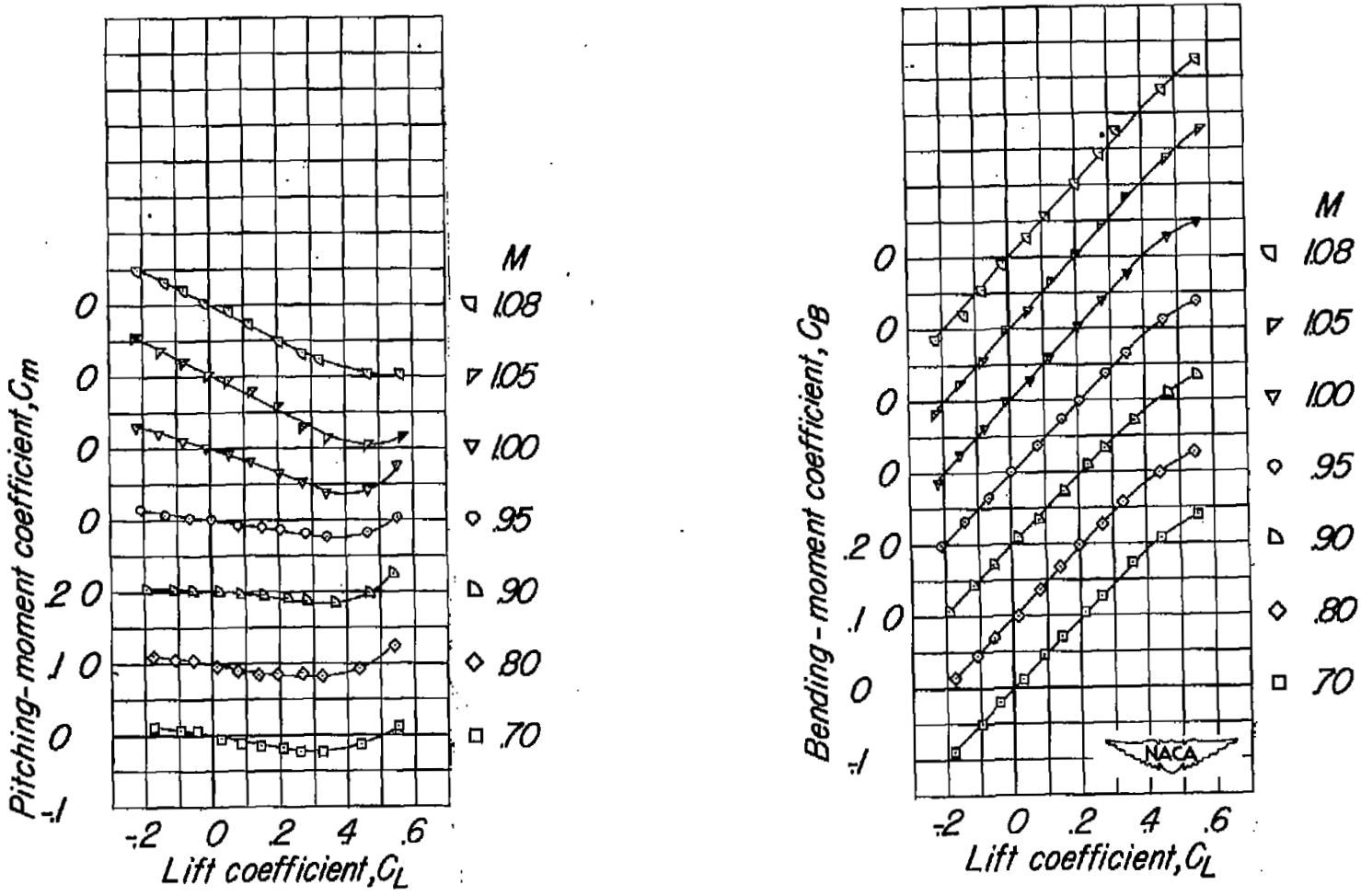

Figure 5.- Concluded.

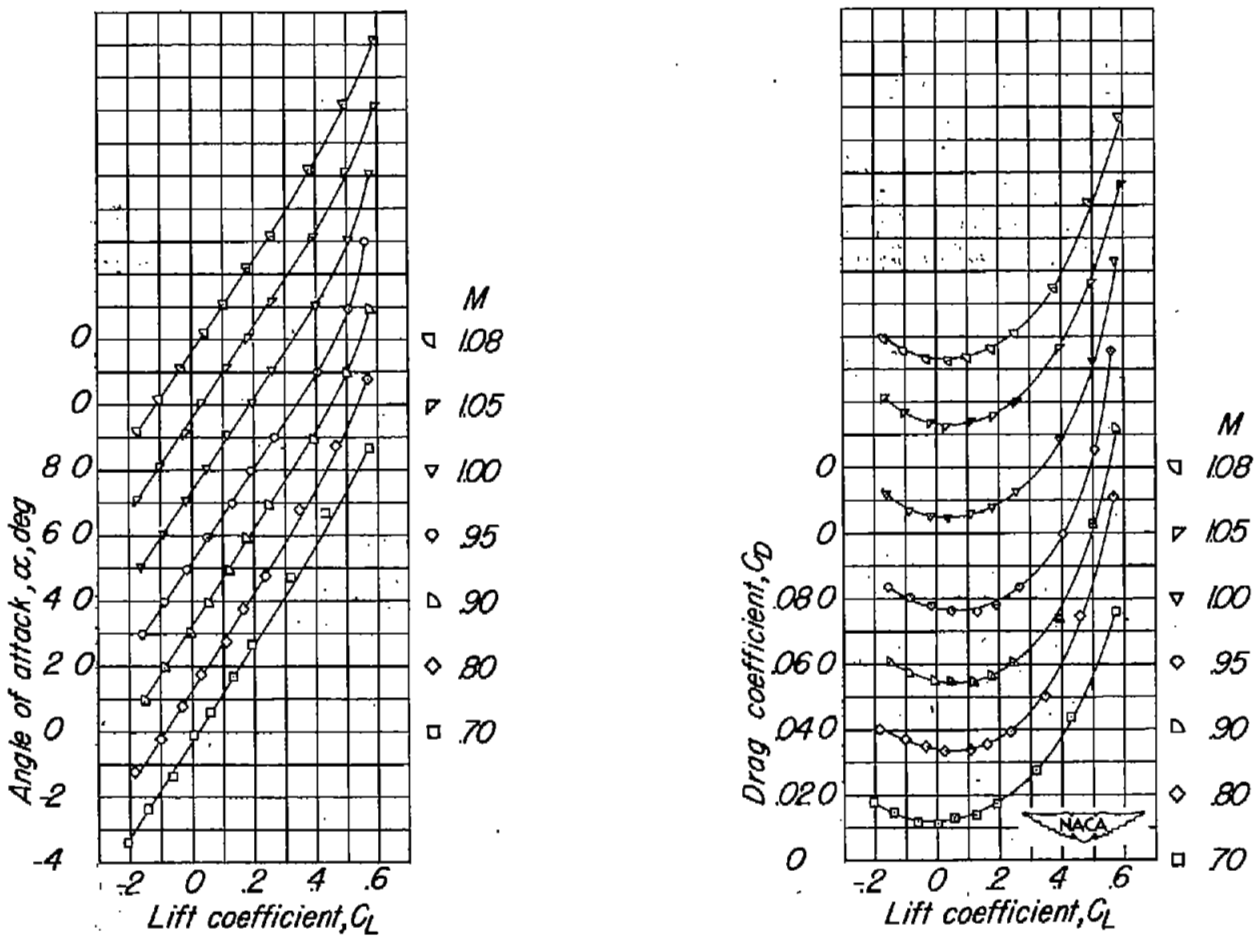

(a) $\frac{y}{b/2} = 0.20$.

Figure 6.- Aerodynamic characteristics of the semispan wing with the nacelle in the rearward chordwise location.

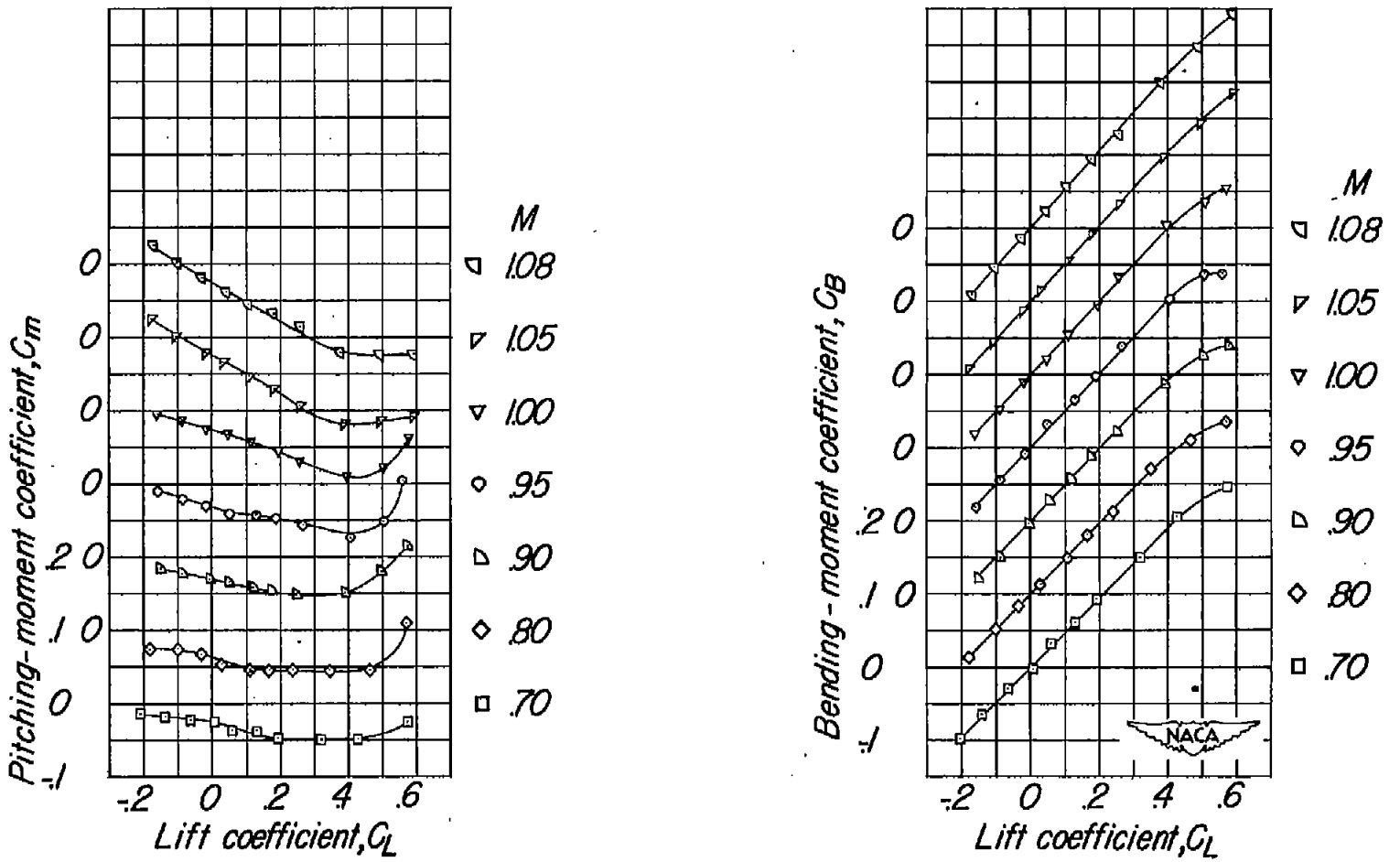

(a) Concluded. $\frac{y}{b/2} = 0.20$.

Figure 6.- Continued.

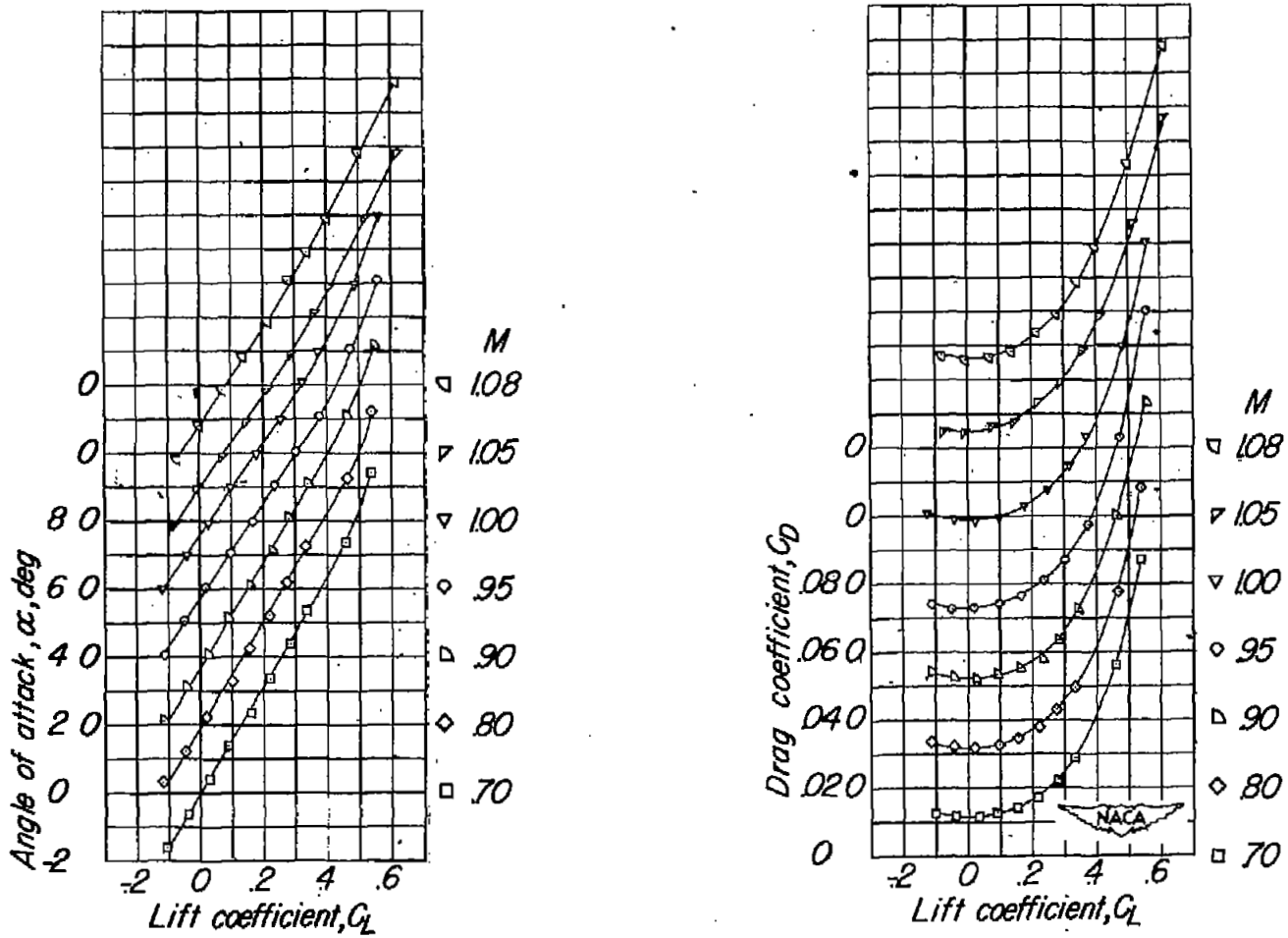

(b) $\frac{y}{b/2} = 0.46$.

Figure 6.- Continued.

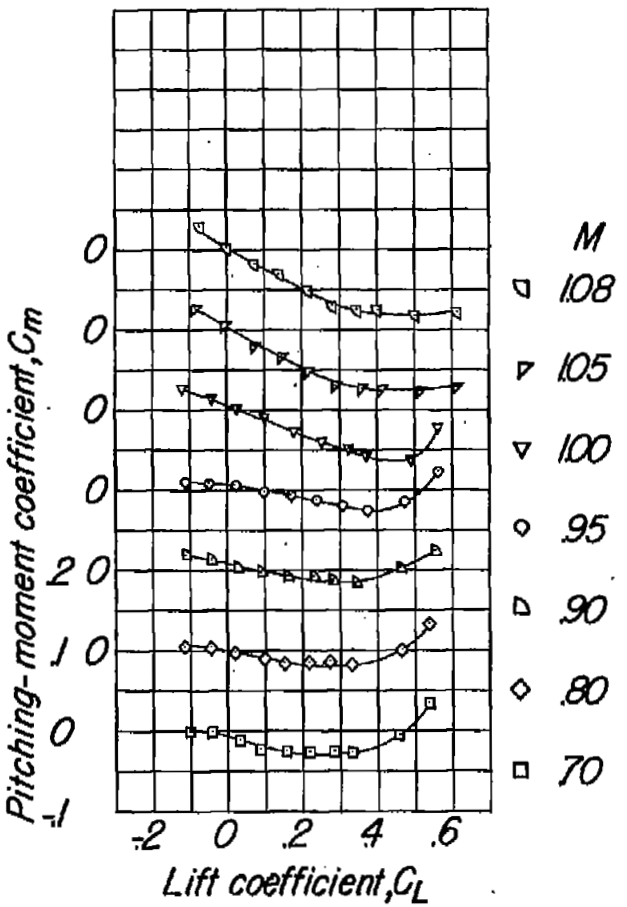

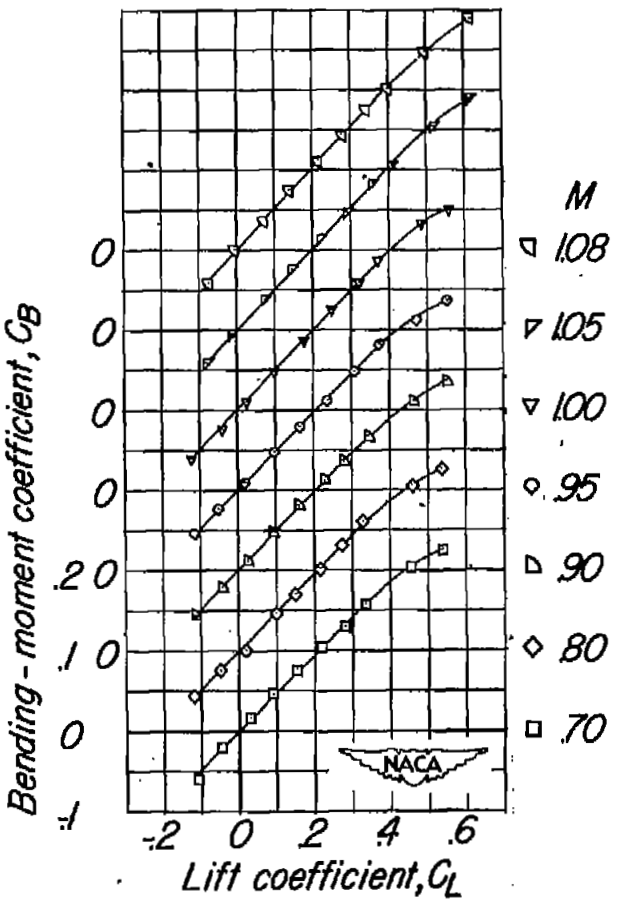

(b) Concluded. $\frac{y}{b/2} = 0.46$.

Figure 6.- Continued.

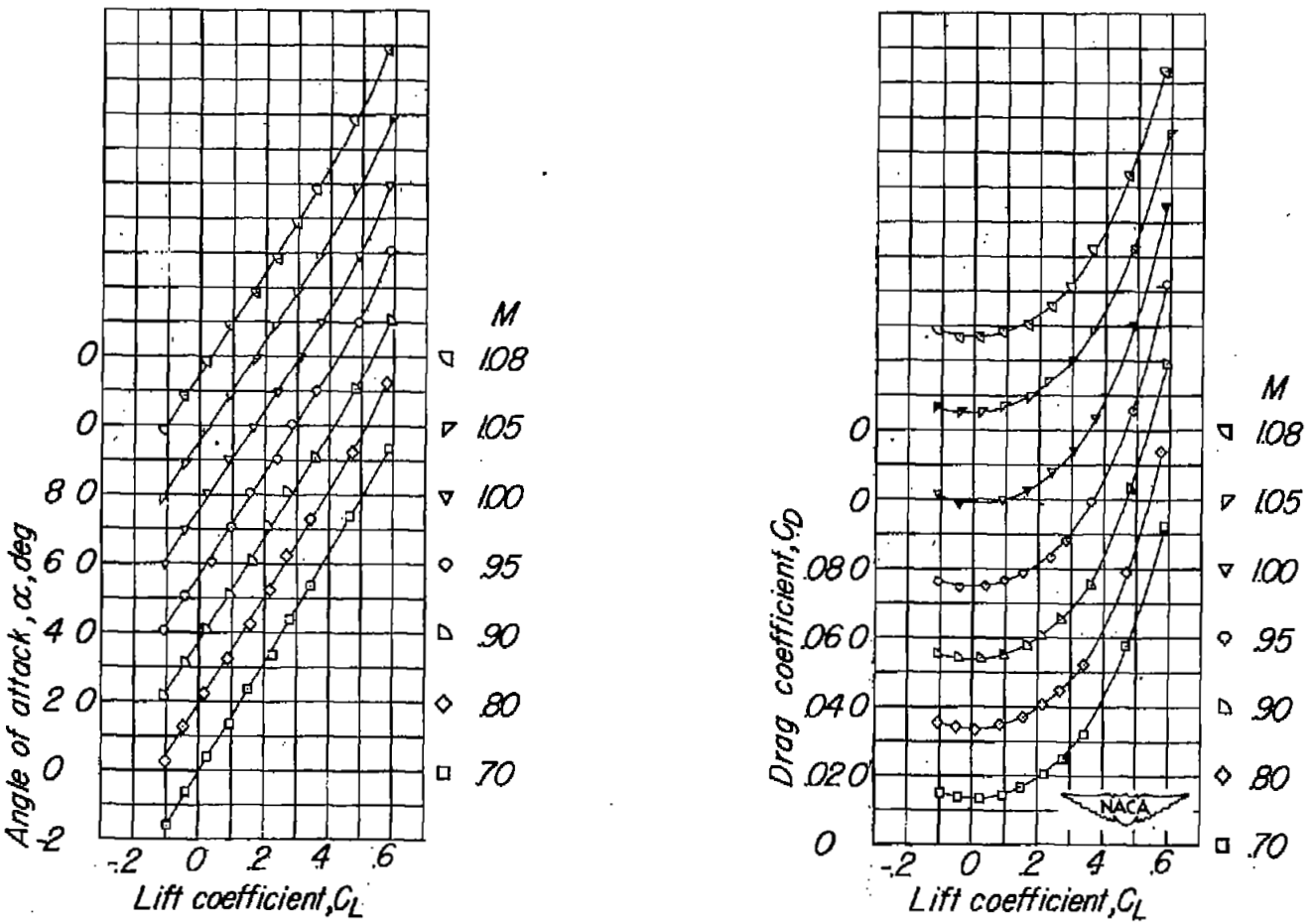

(c) $\frac{y}{b/2} = 0.70$.

Figure 6.- Continued.

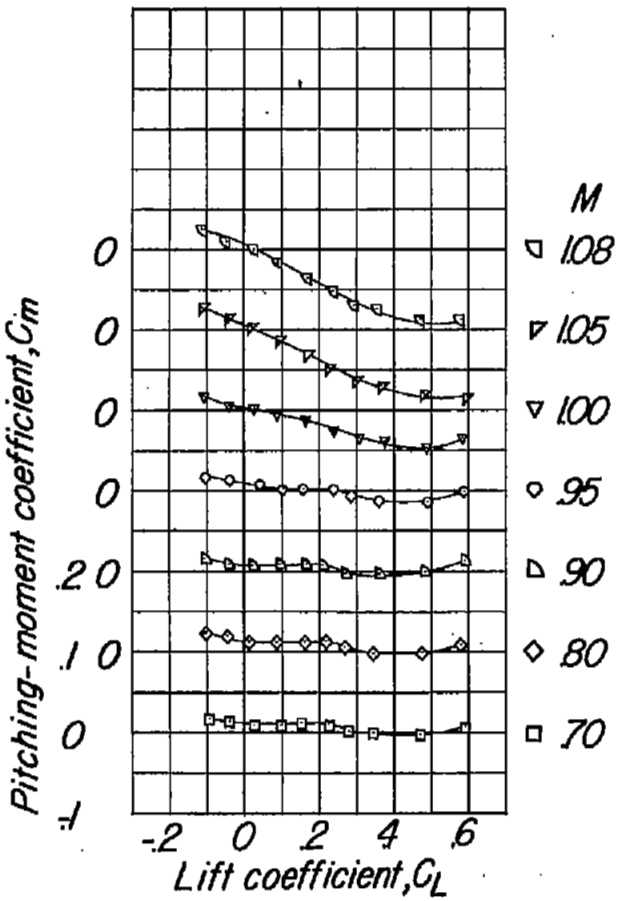

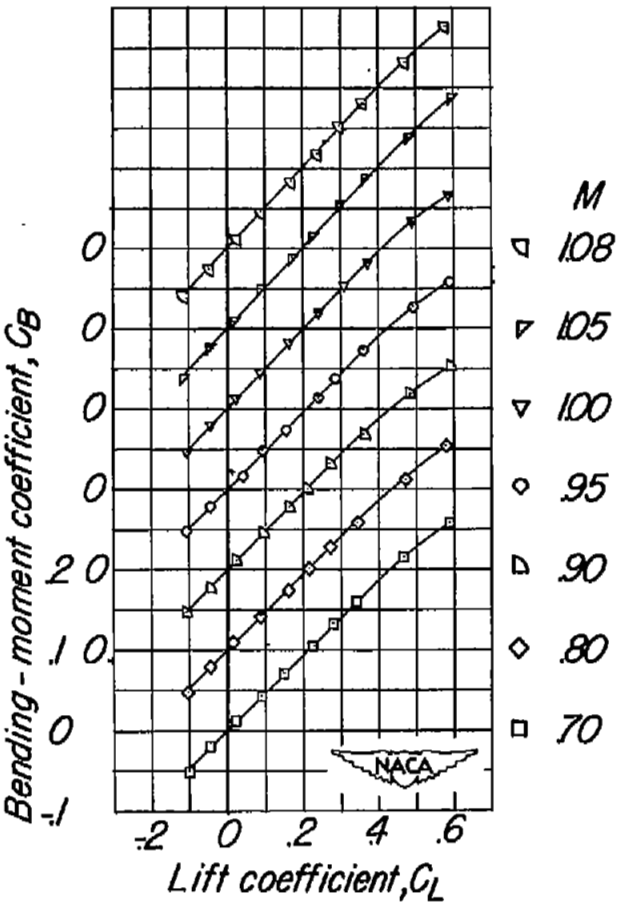

(c) Concluded. $\frac{y}{b/2} = 0.70$.

Figure 6.- Continued.

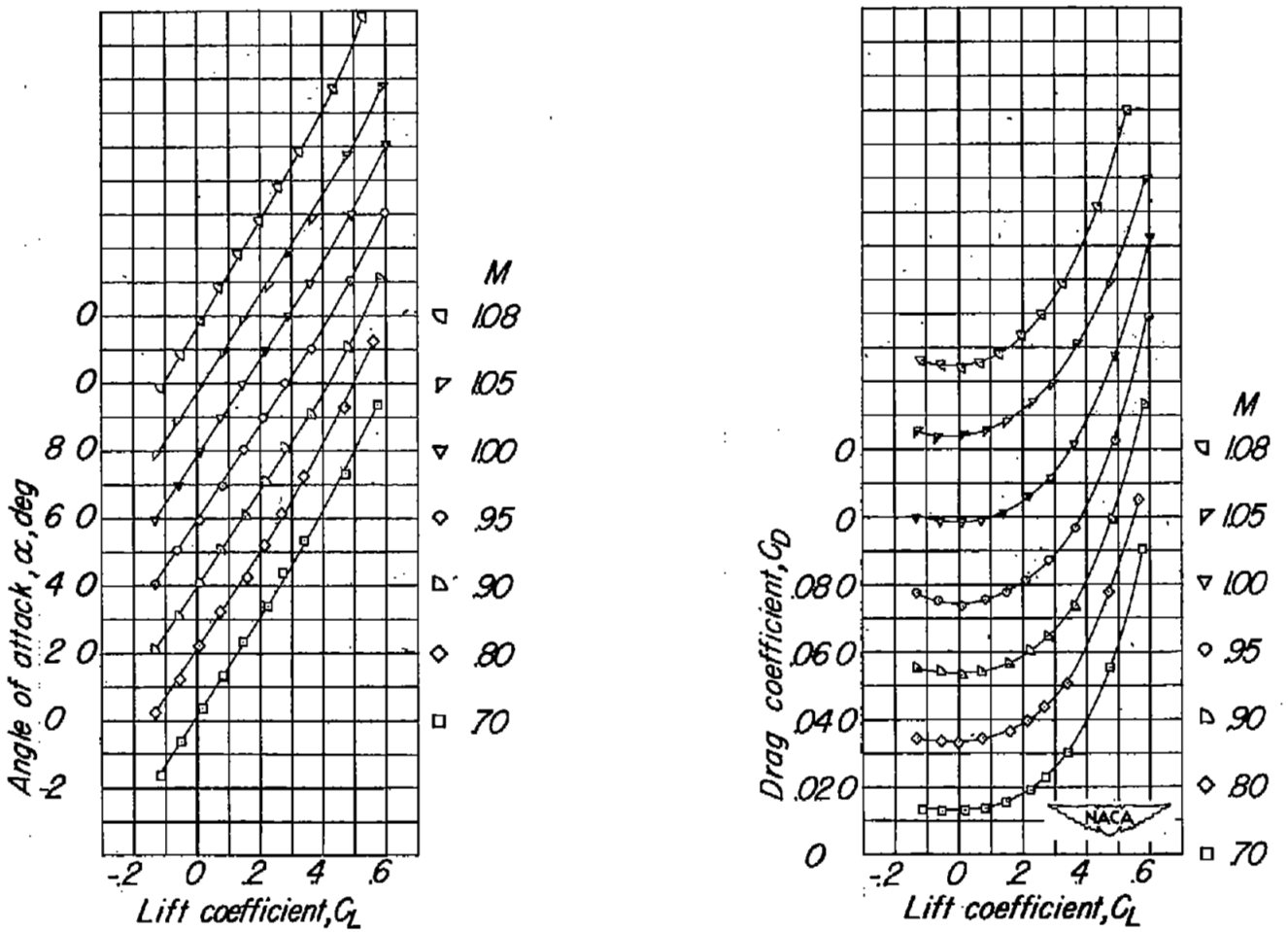

(d) $\frac{y}{b/2} = 0.96$.

Figure 6.- Continued.

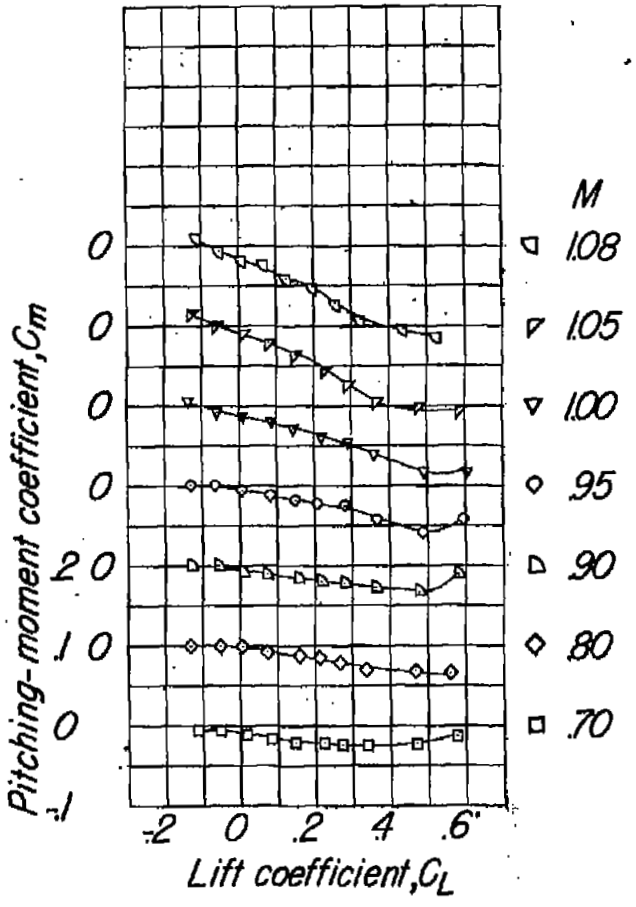

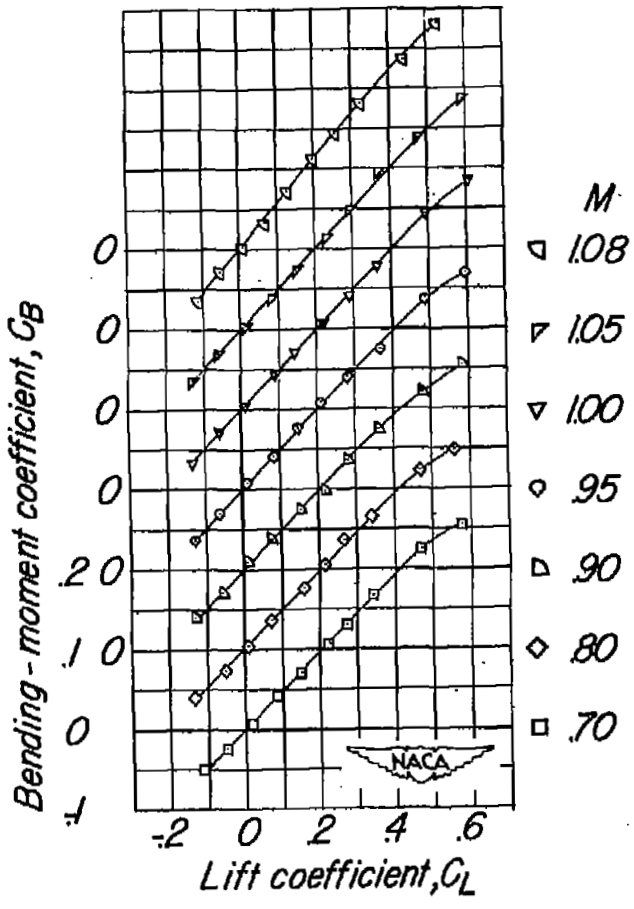

(d) Concluded. $\frac{y}{b/2} = 0.96$.

Figure 6.- Concluded.

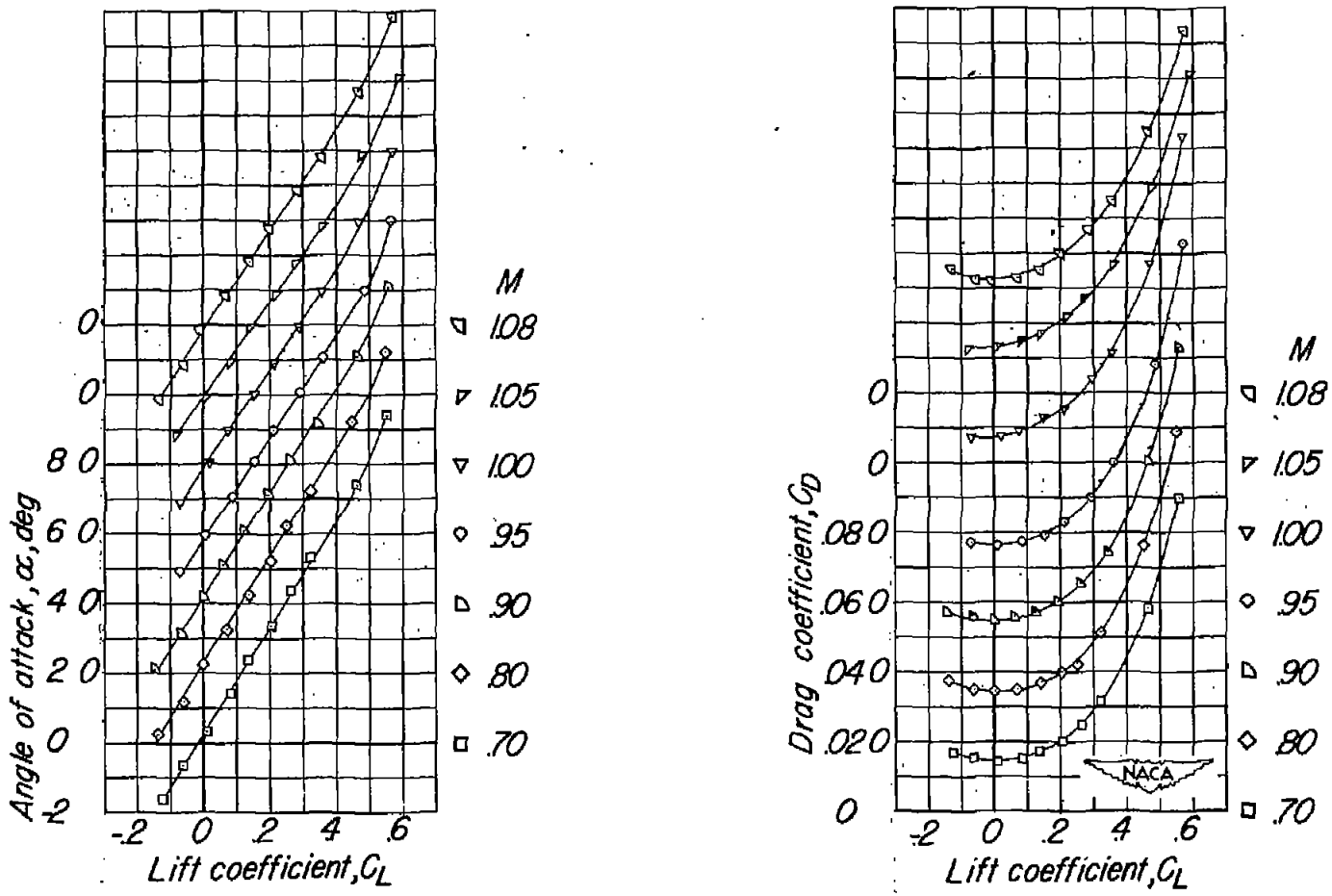

(a) $\frac{y}{b/2} = 0.20$.

Figure 7.- Aerodynamic characteristics of the semispan wing with the nacelle in the intermediate chordwise location.

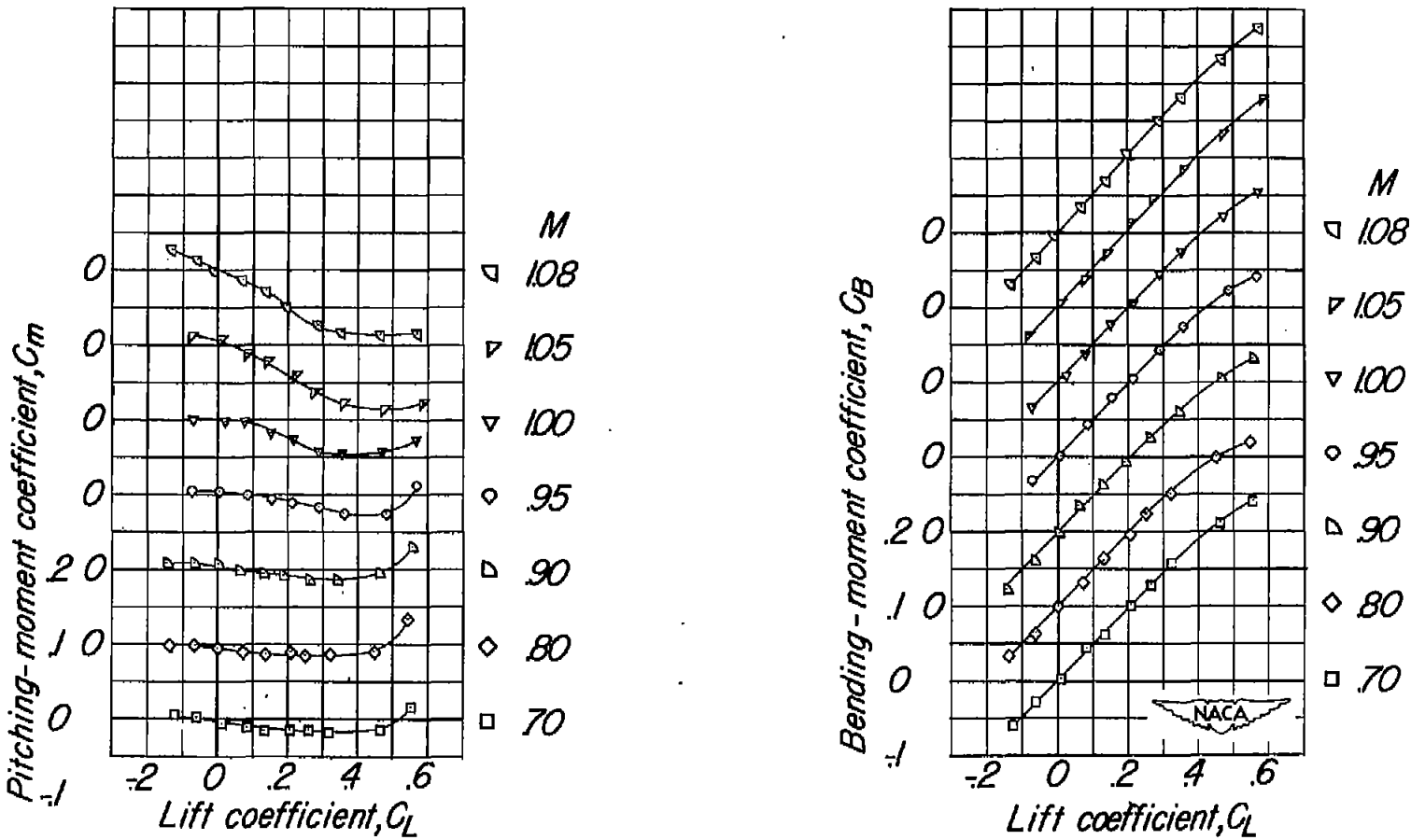

(a) Concluded. $\frac{y}{b/2} = 0.20$.

Figure 7.- Continued.

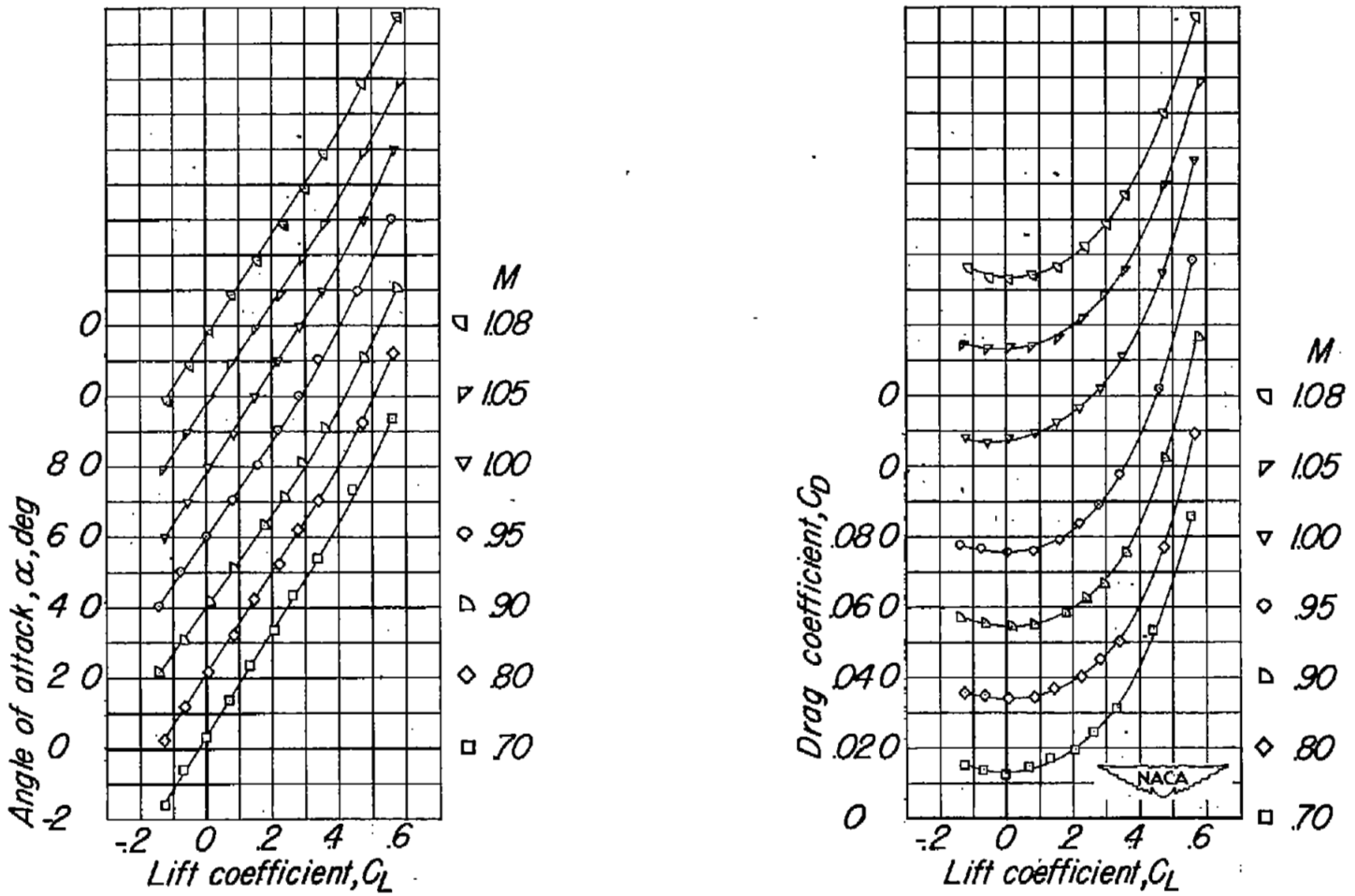

(b) $\frac{y}{b/2} = 0.46$.

Figure 7.- Continued.

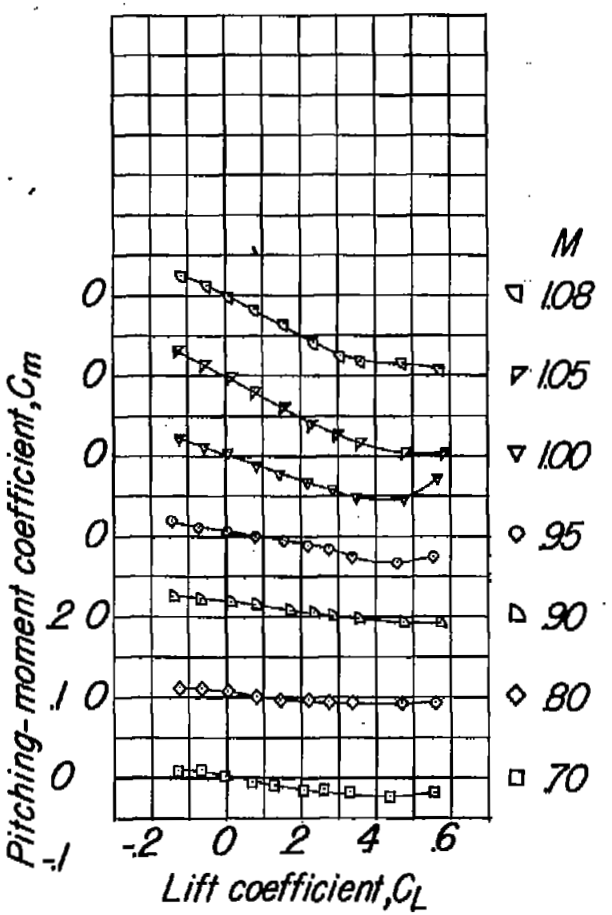

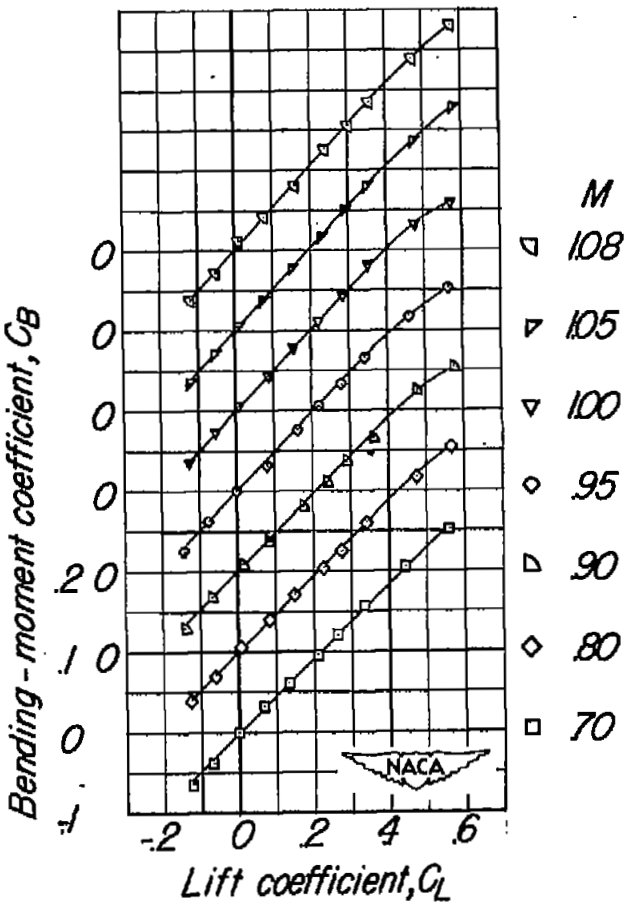

(b) Concluded. $\frac{y}{b/2} = 0.46$.

Figure 7.- Continued.

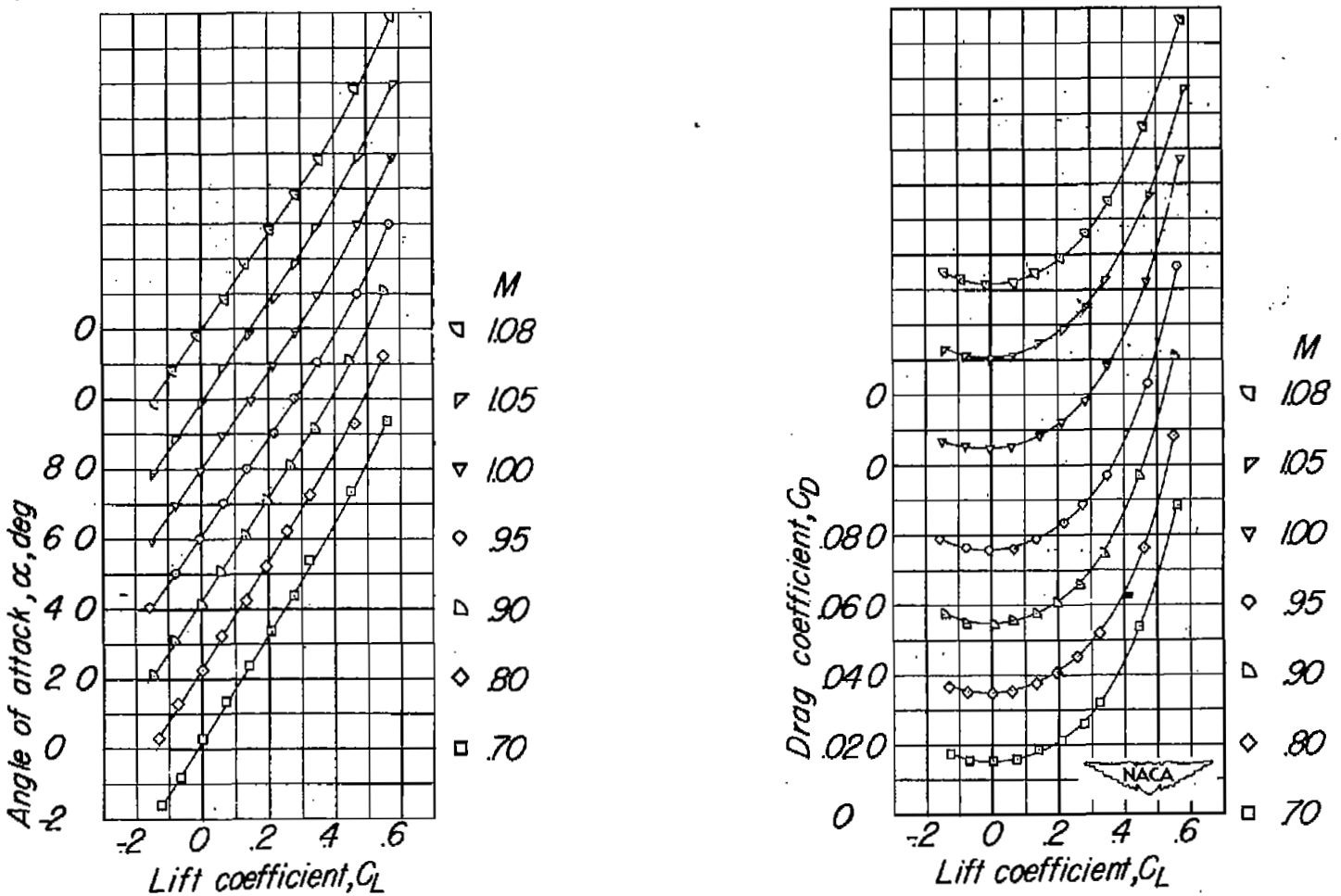

(c) $\frac{y}{b/2} = 0.70$.

Figure 7.- Continued.

(c) Concluded. $\frac{y}{b/2} = 0.70$.

Figure 7.- Continued.

(d) $\frac{y}{b/2} = 0.96$.

Figure 7.- Continued.

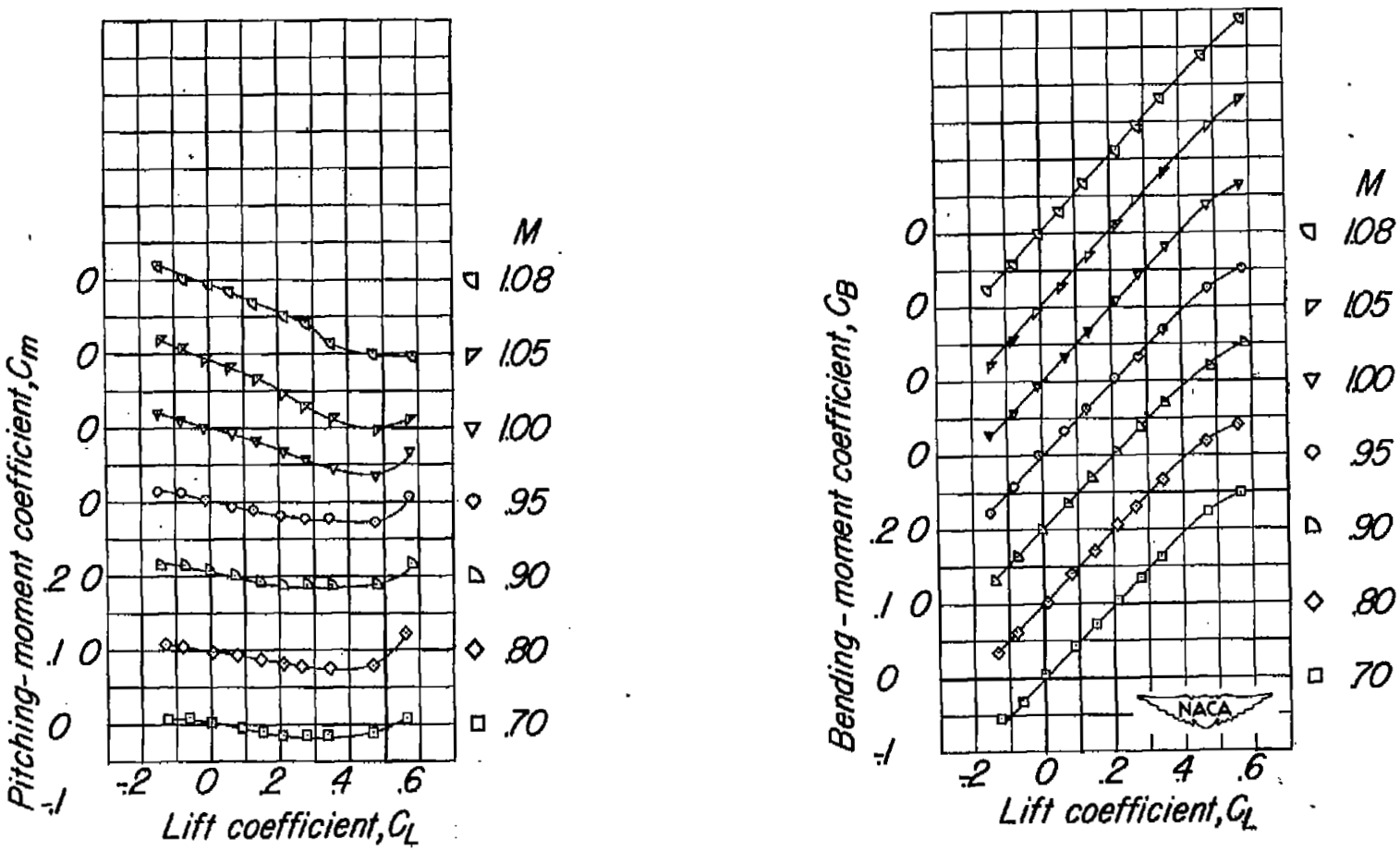

(d) Concluded. $\frac{y}{b/2} = 0.96$.

Figure 7.- Concluded.

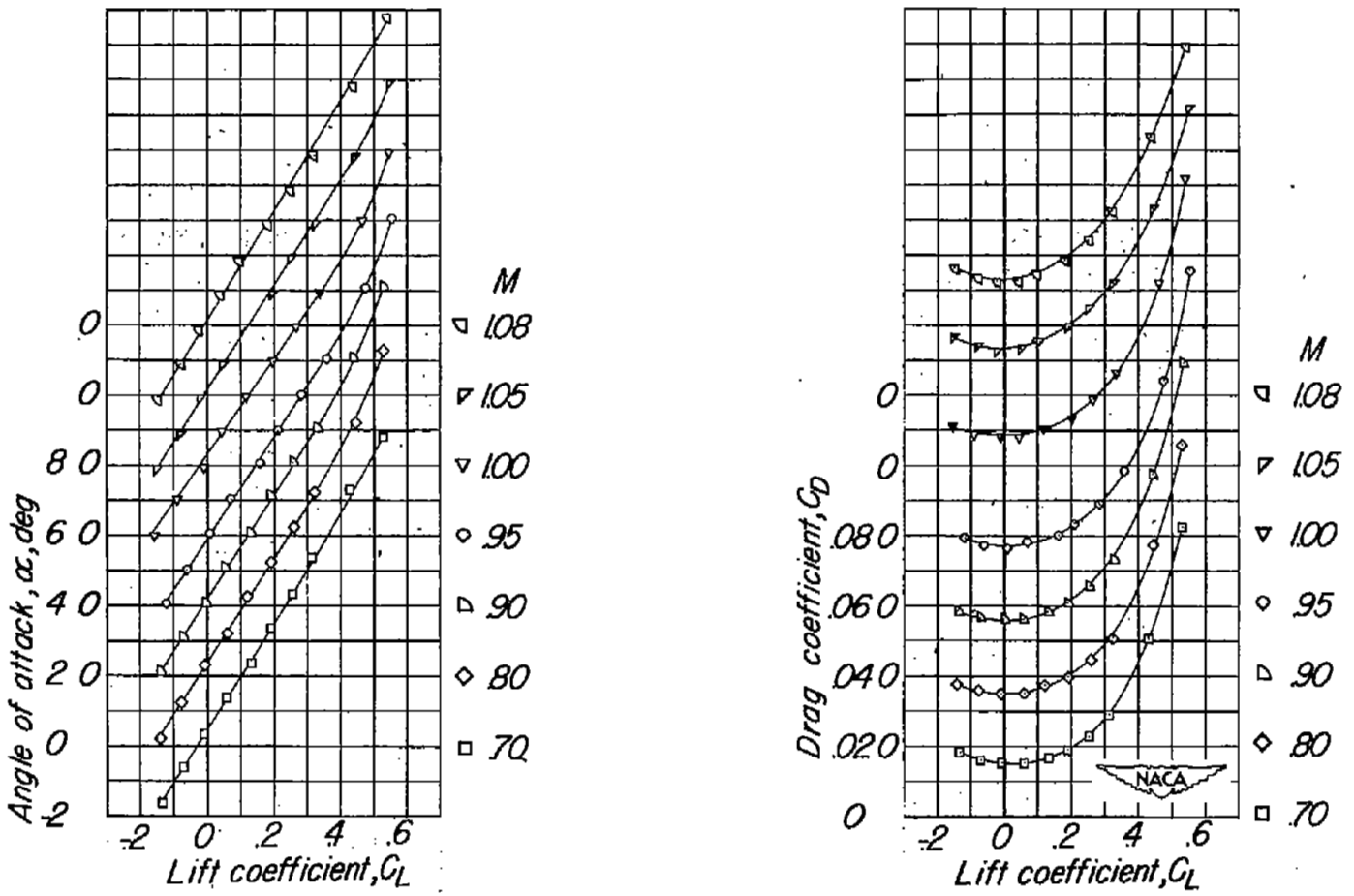

(a) $\frac{y}{b/2} = 0.20$.

Figure 8.- Aerodynamic characteristics of the semispan wing with the nacelle in the forward chordwise location.

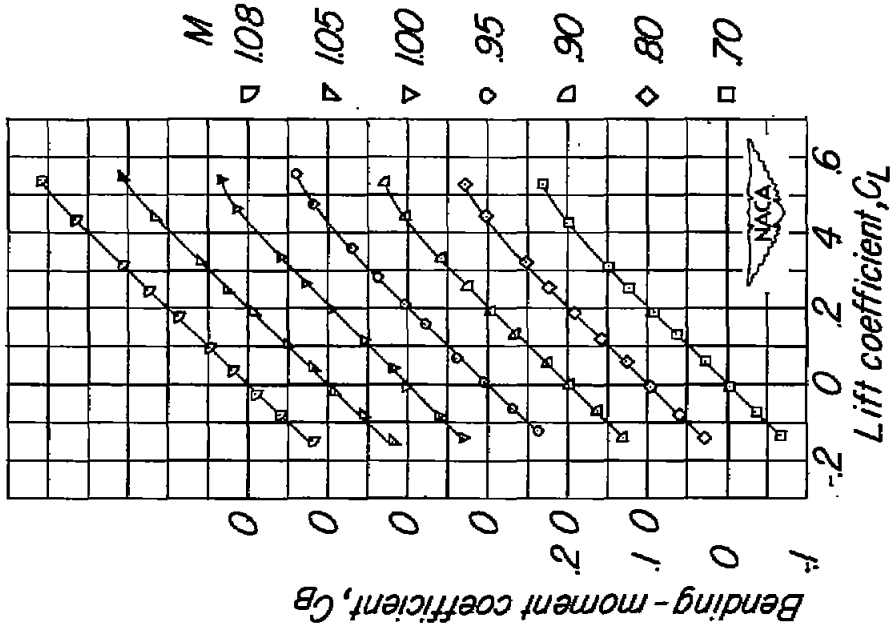

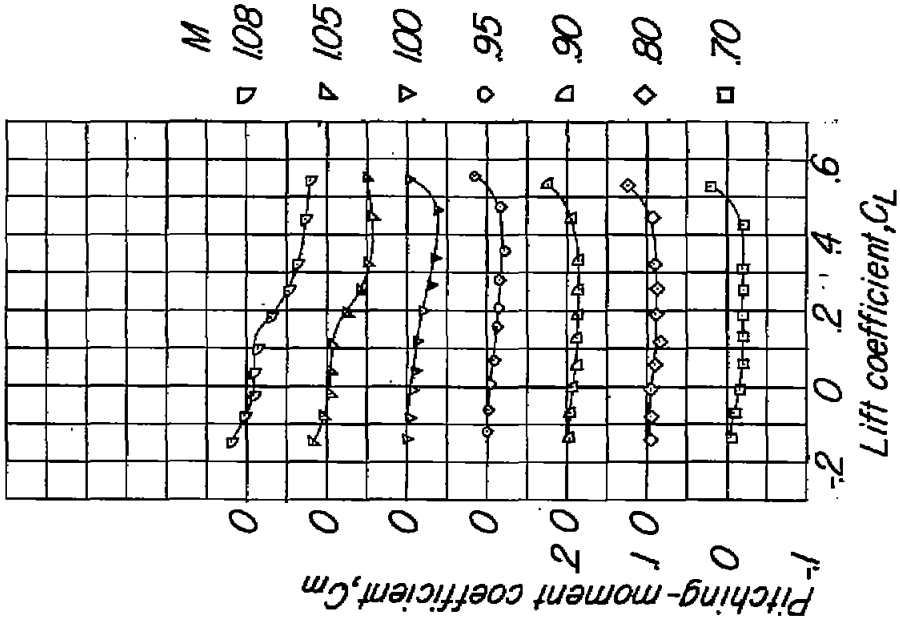

(a) Concluded. $\frac{y}{b/2} = 0.20$.

Figure 8.- Continued.

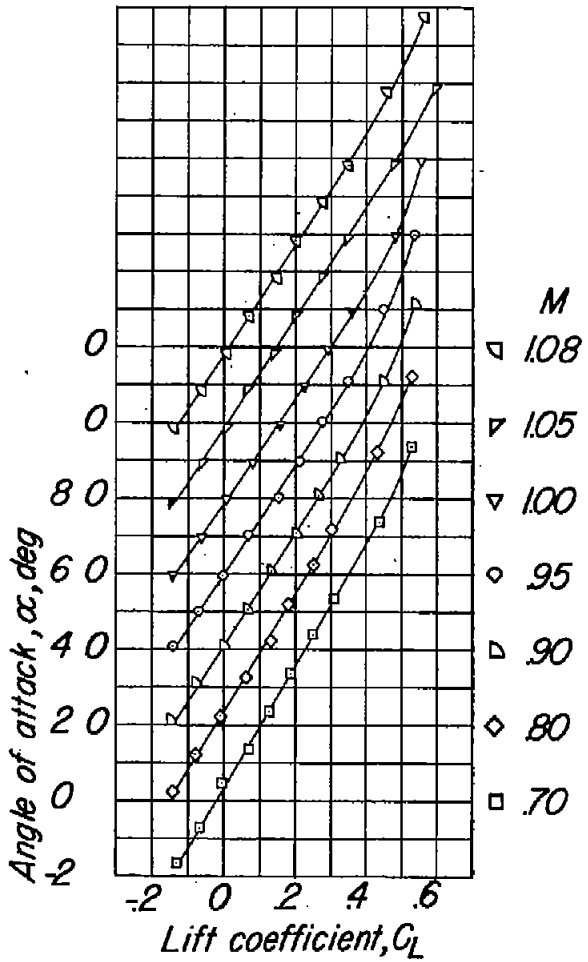

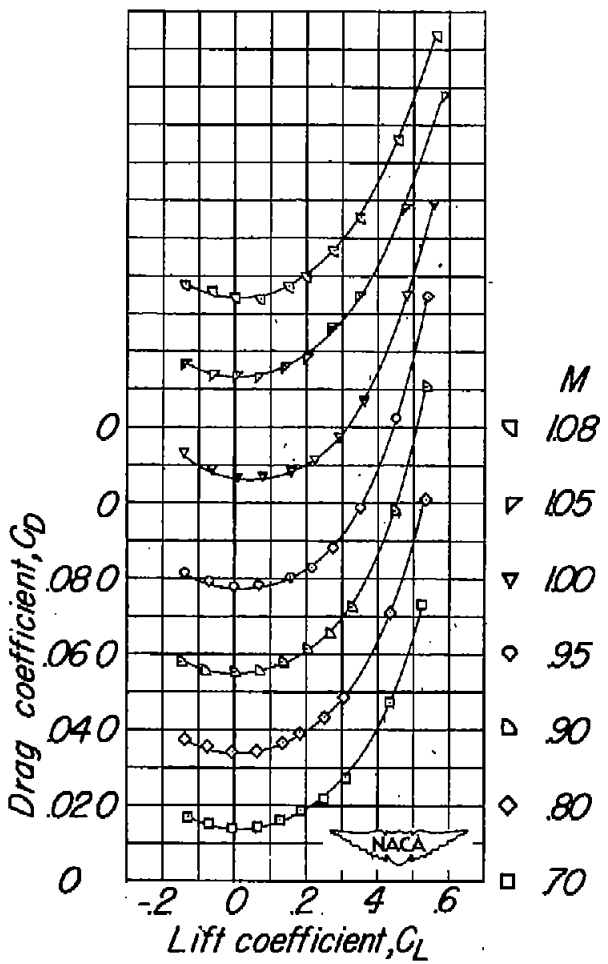

(b) $\frac{y}{b/2} = 0.46$.

Figure 8.- Continued.

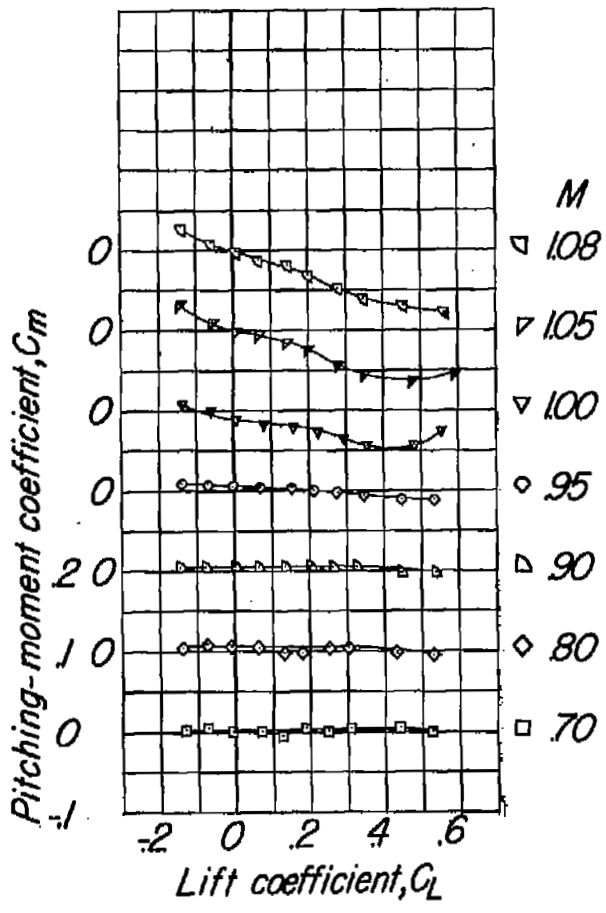

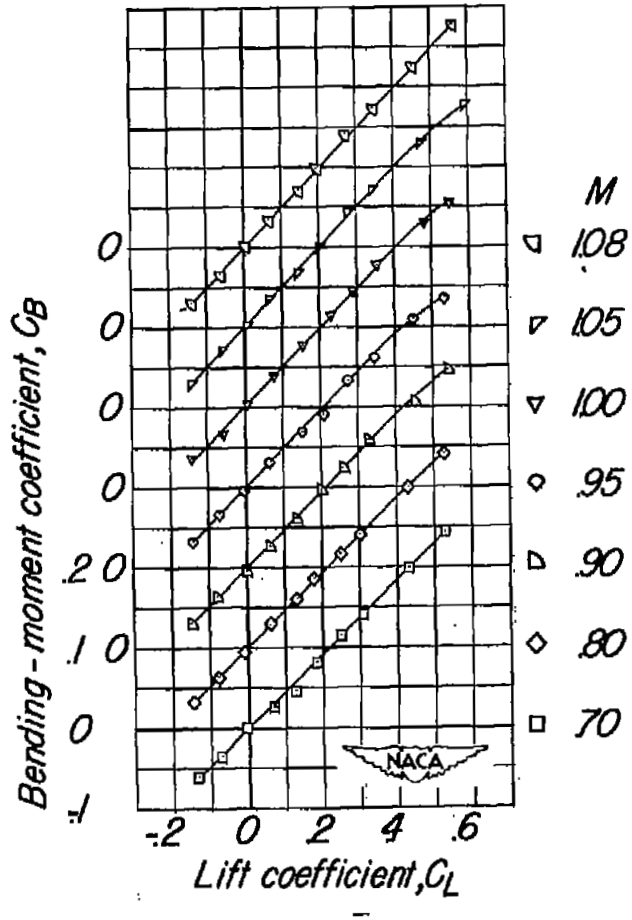

(b) Concluded. $\frac{y}{b/2} = 0.46$.

Figure 8.- Continued.

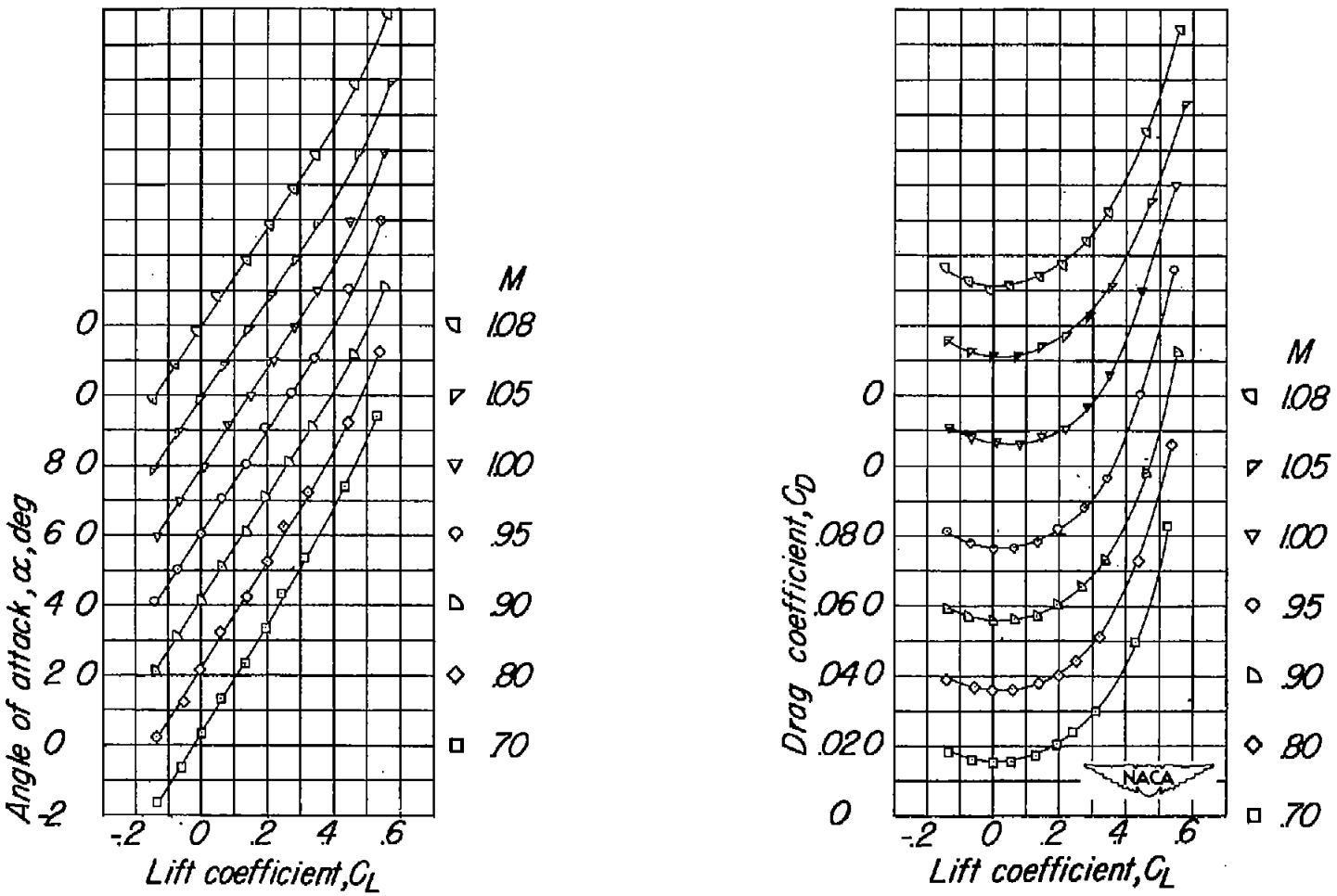

(c) $\frac{y}{b/2} = 0.70$.

Figure 8.- Continued.

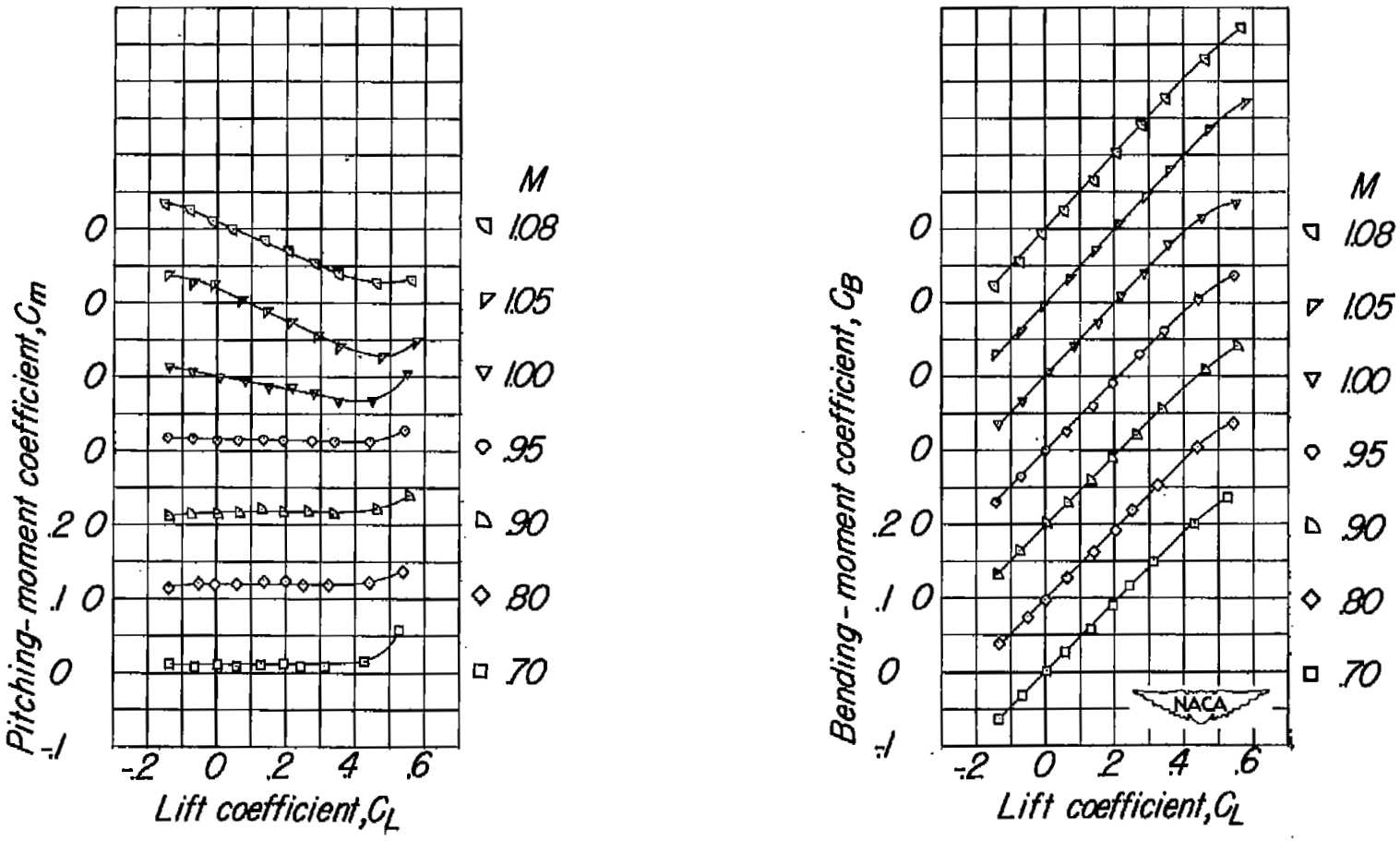

(c) Concluded. $\frac{y}{b/2} = 0.70$.

Figure 8.- Continued.

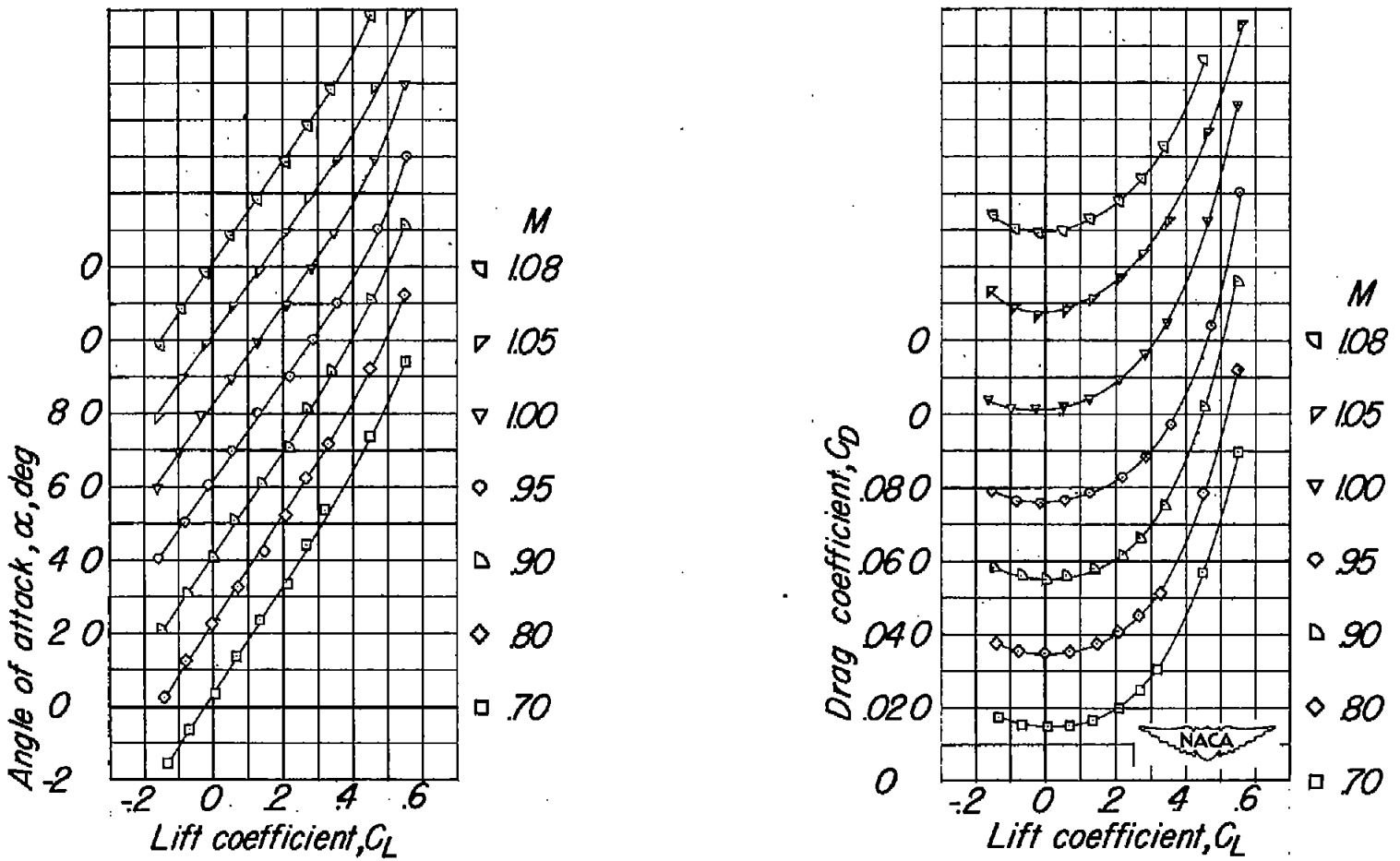

(d) $\frac{y}{b/2} = 0.96$.

Figure 8.- Continued.

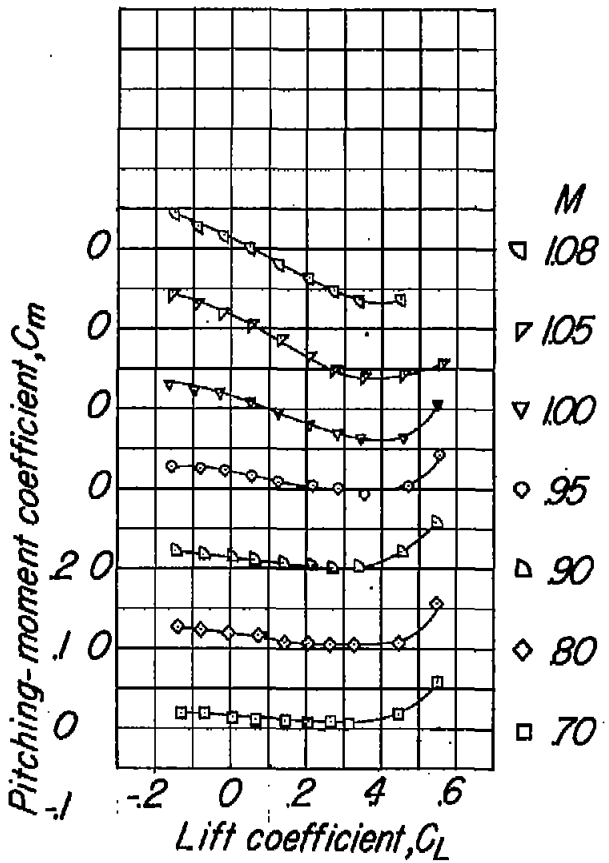

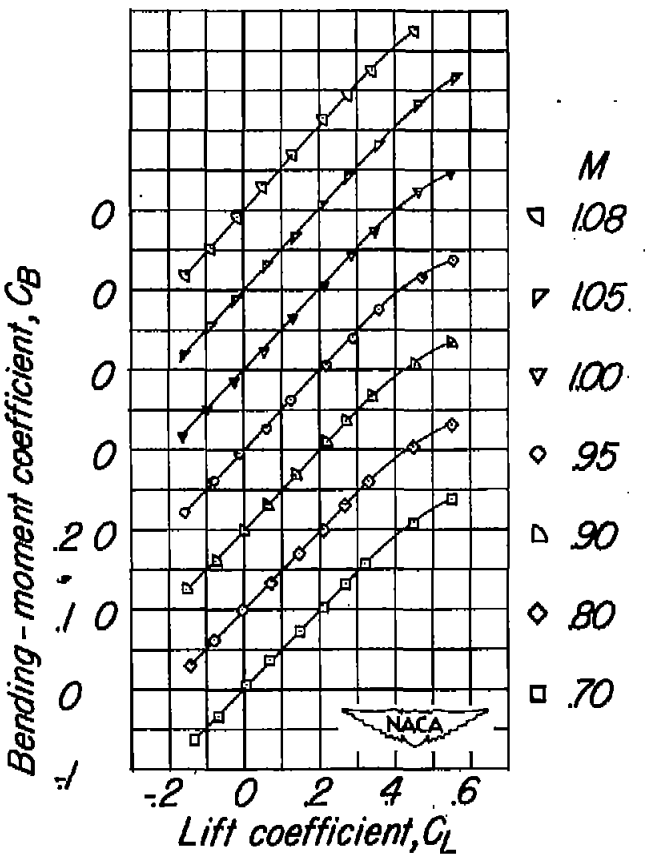

(d) Concluded. $\frac{y}{b/2} = 0.96$.

Figure 8.- Concluded.

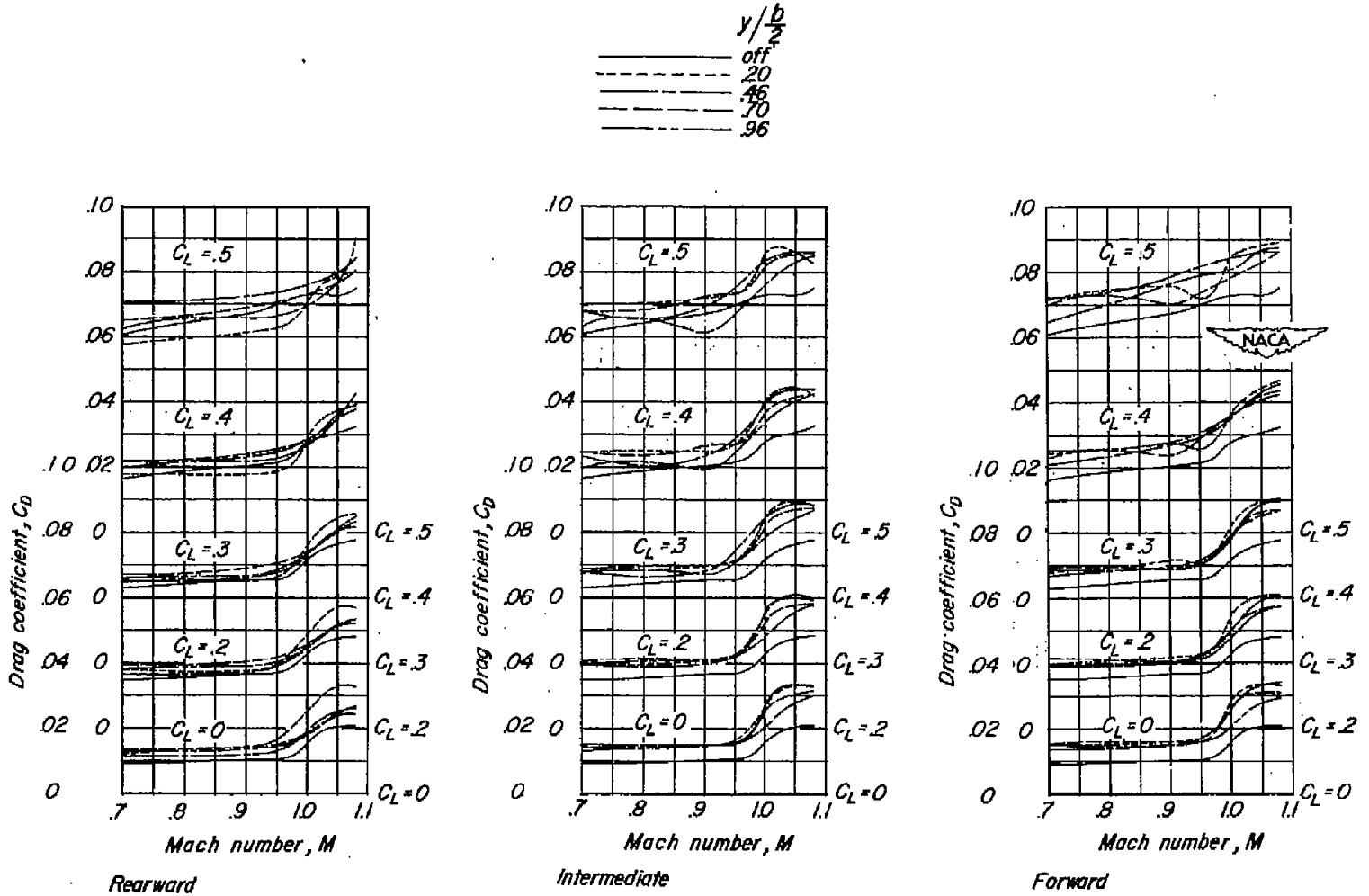

Figure 9.- Variation of drag coefficient with Mach number of the semispan wing alone and the wing with the nacelle in several spanwise and chordwise locations.

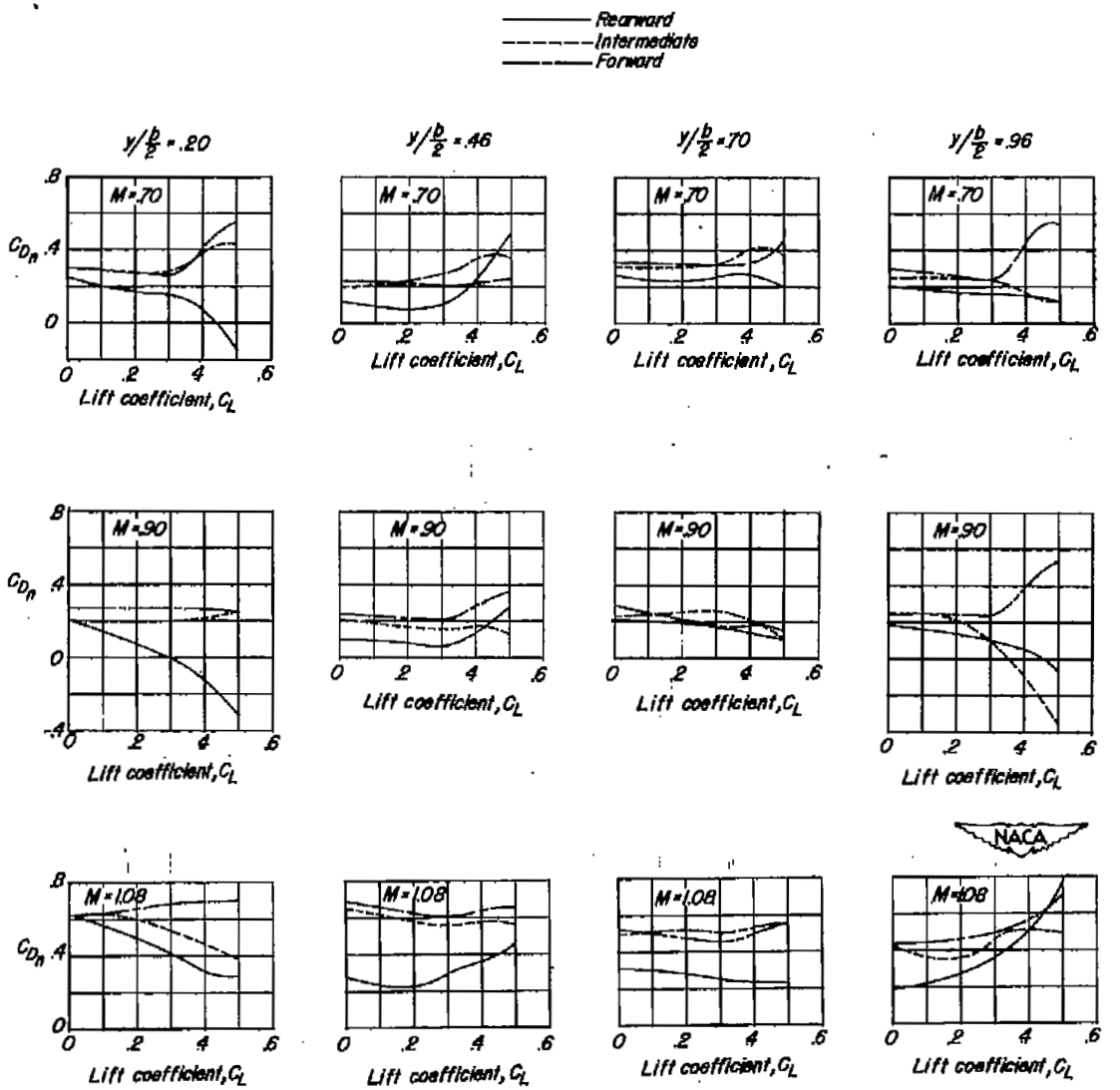

Figure 10.- Variation of the nacelle drag coefficients with lift coefficient.

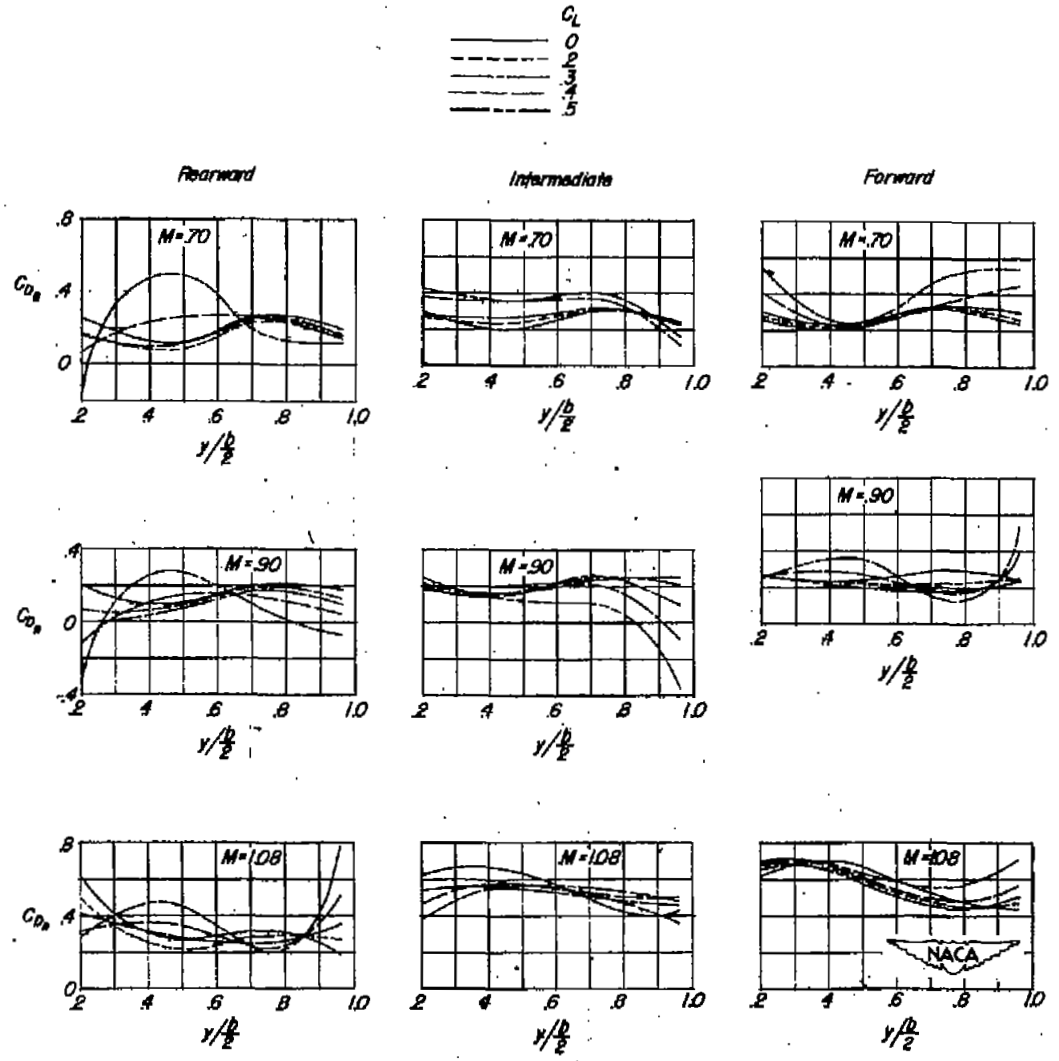

Figure 11.- Variation of the nacelle drag coefficient with nacelle spanwise location.

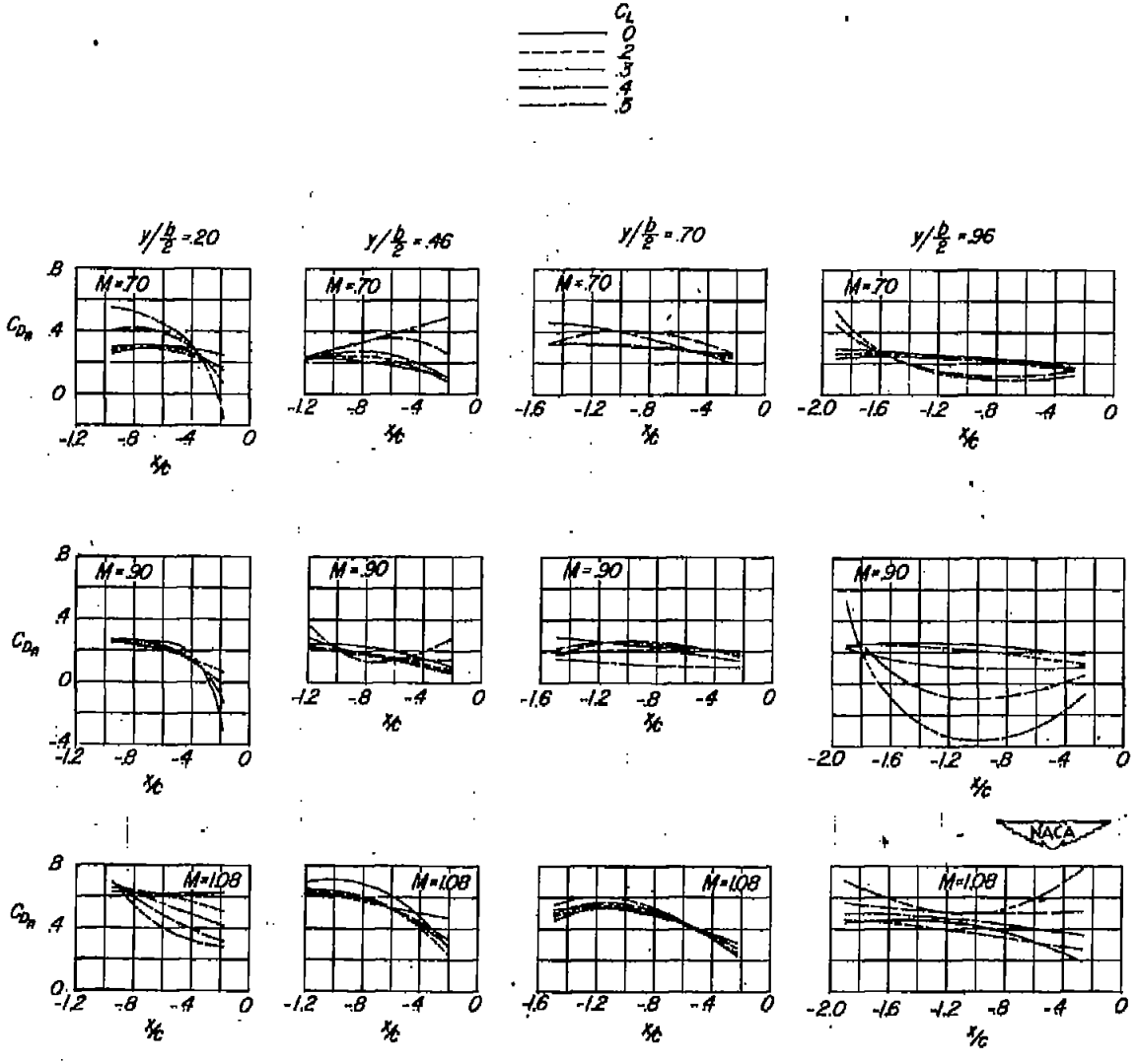

Figure 12.- Variation of the nacelle drag coefficient with nacelle chordwise location.

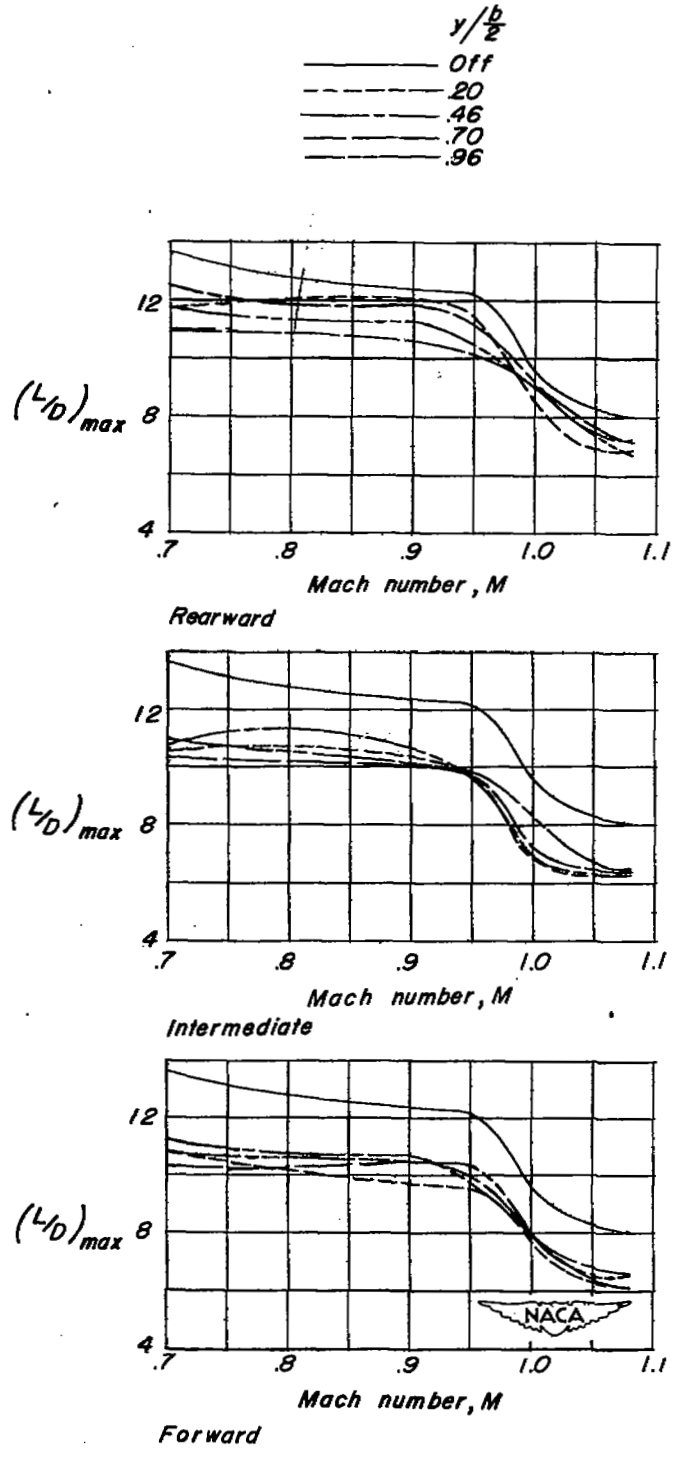

Figure 13.- Variation of the maximum lift-drag ratios with Mach number.

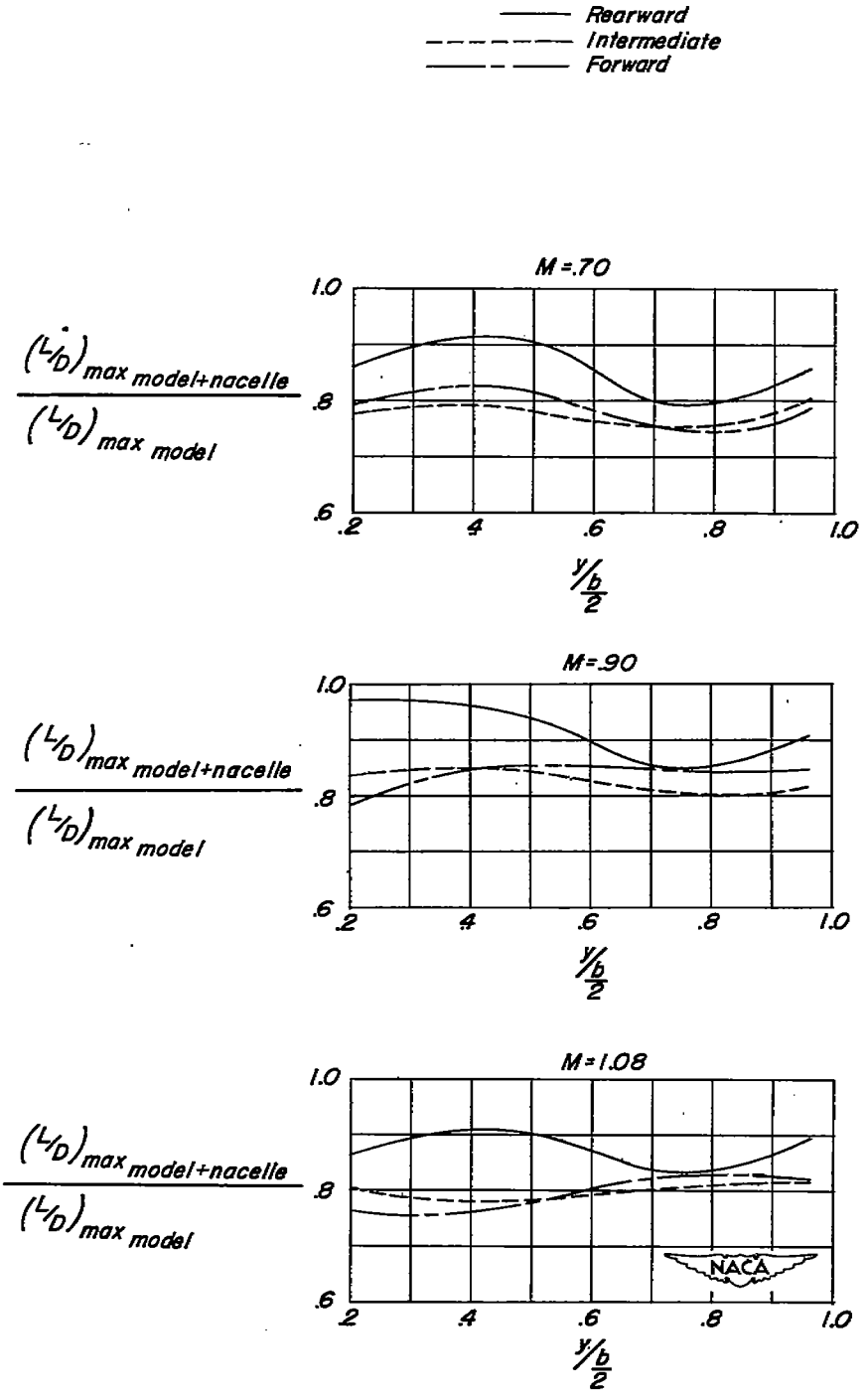

Figure 14.- Variation of the ratios of the maximum lift-drag ratio of the model with nacelle to the maximum lift-drag ratio of the model without nacelle with nacelle spanwise location.

[redacted]

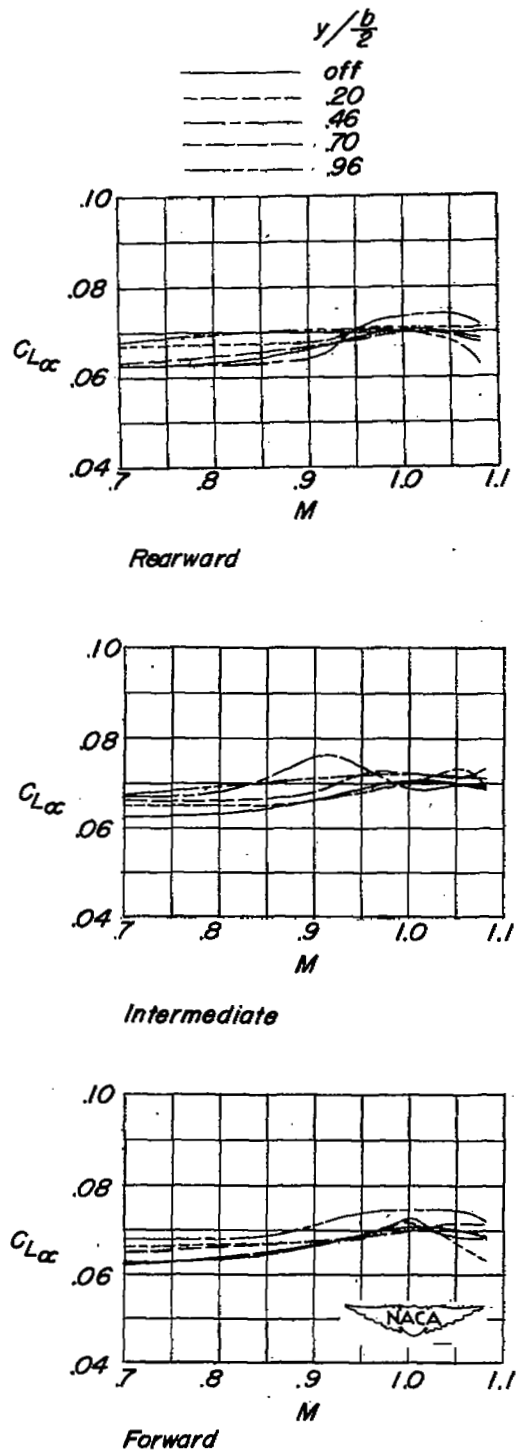

Figure 15.- Variation of the lift-curve slopes with Mach number.

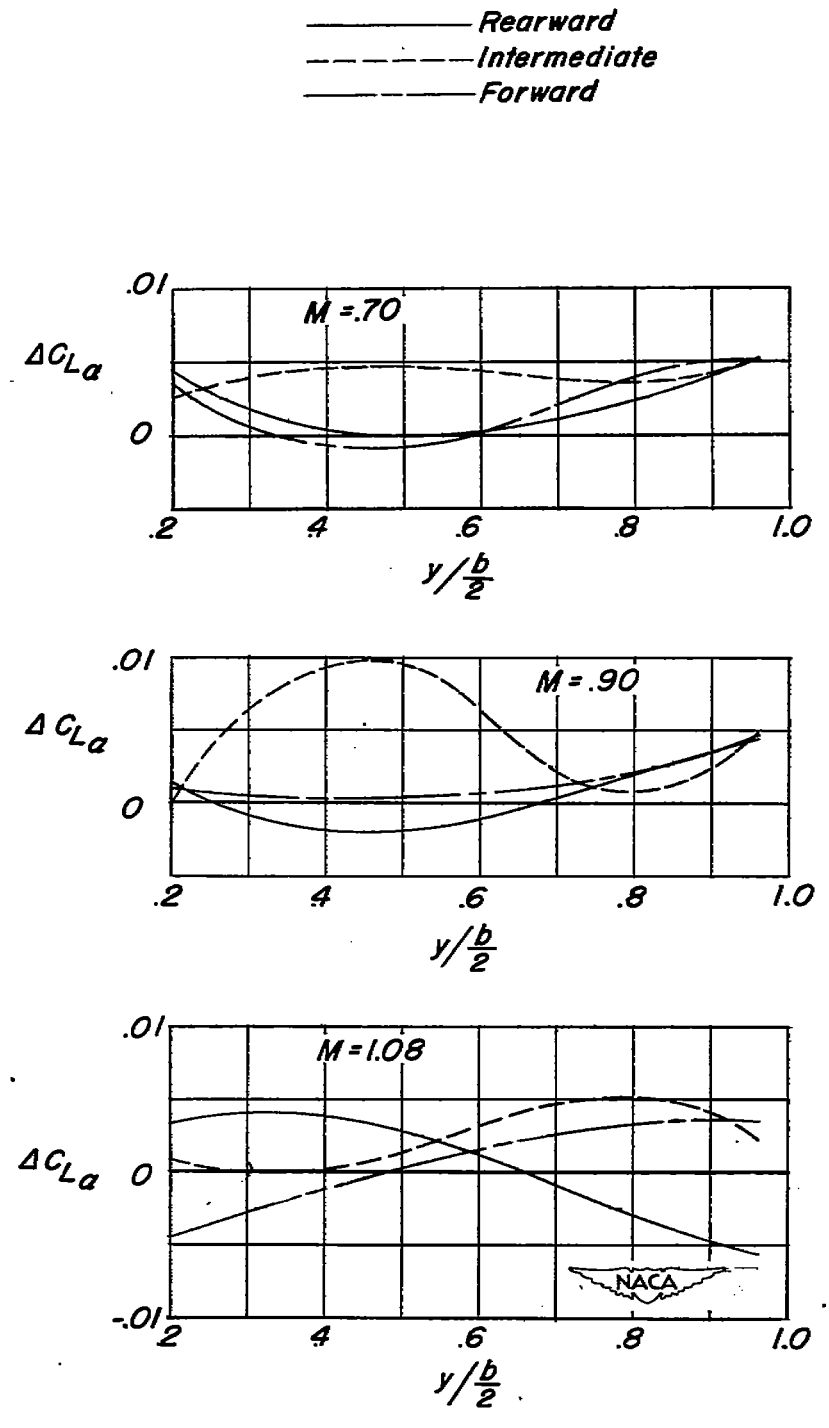

Figure 16.- Variation of the increments in lift-curve slopes with nacelle spanwise location.

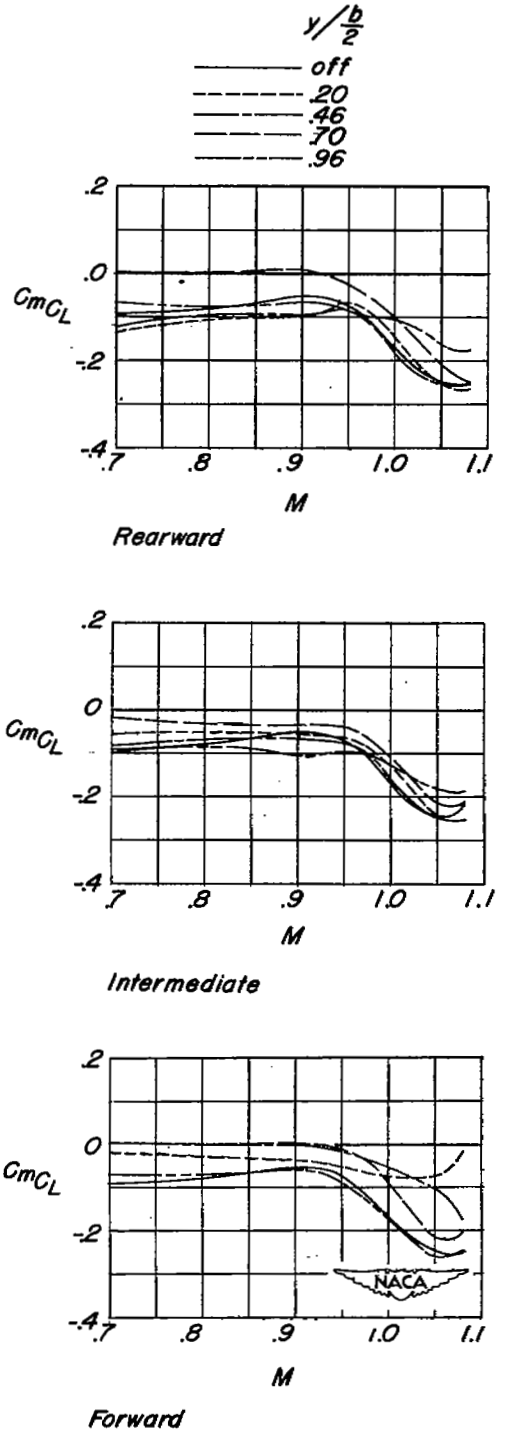

Figure 17.- Variation of the pitching-moment-curve slopes with Mach number.

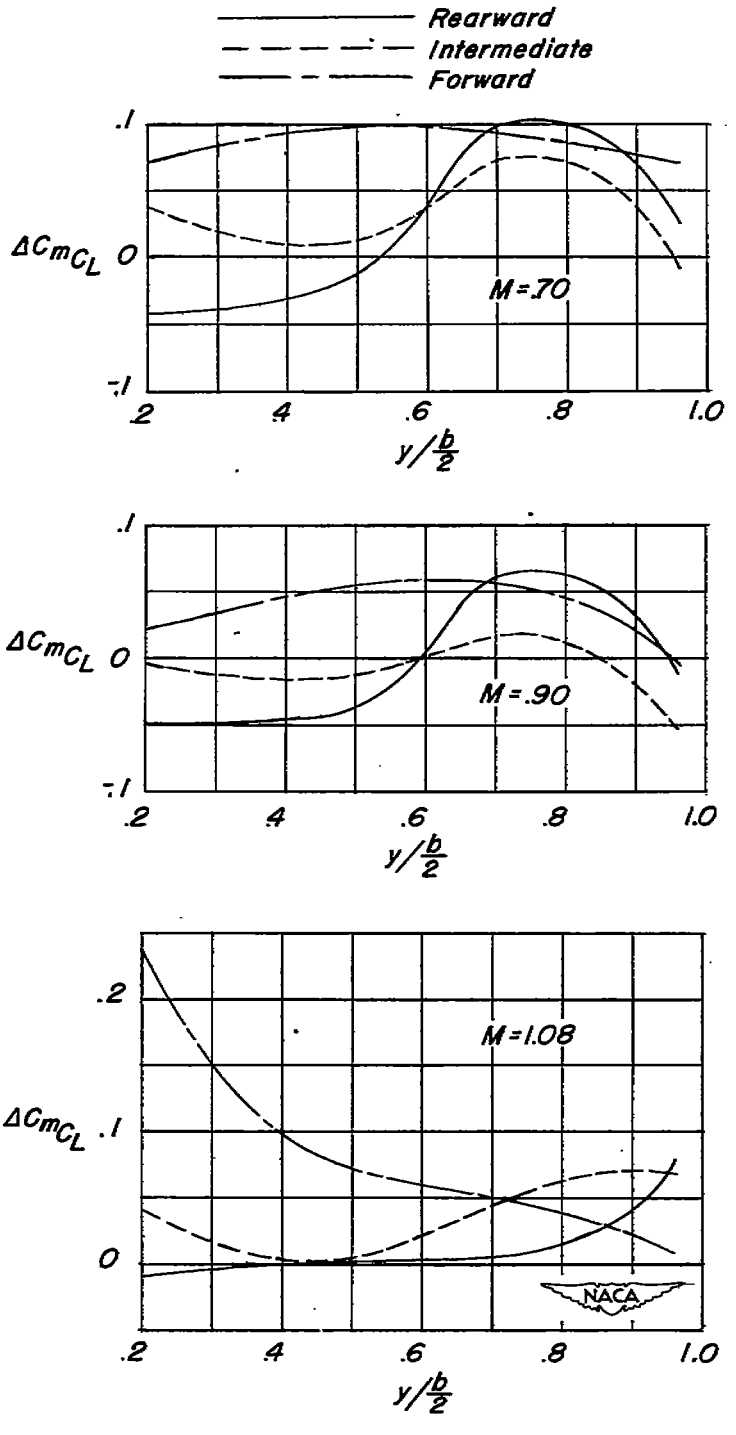

Figure 18.- Variation of the increments in pitching-moment-curve slopes with nacelle spanwise location as obtained from figure 17.

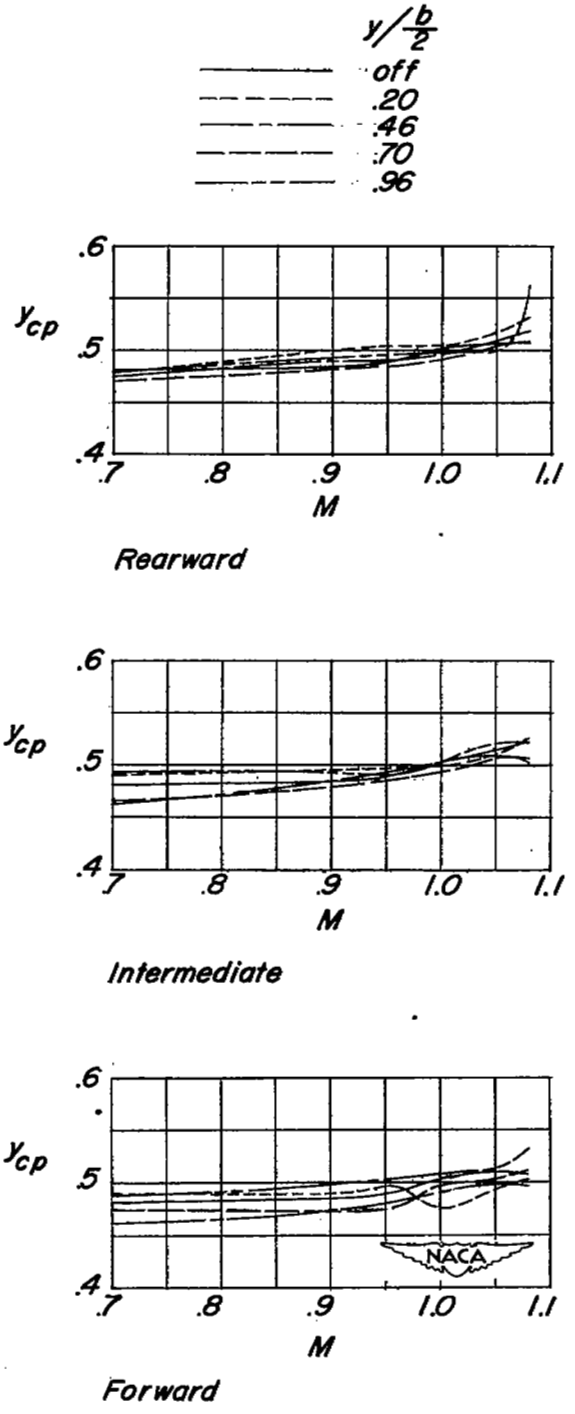

Figure 19.- Variation of the lateral center-of-pressure locations with Mach number.

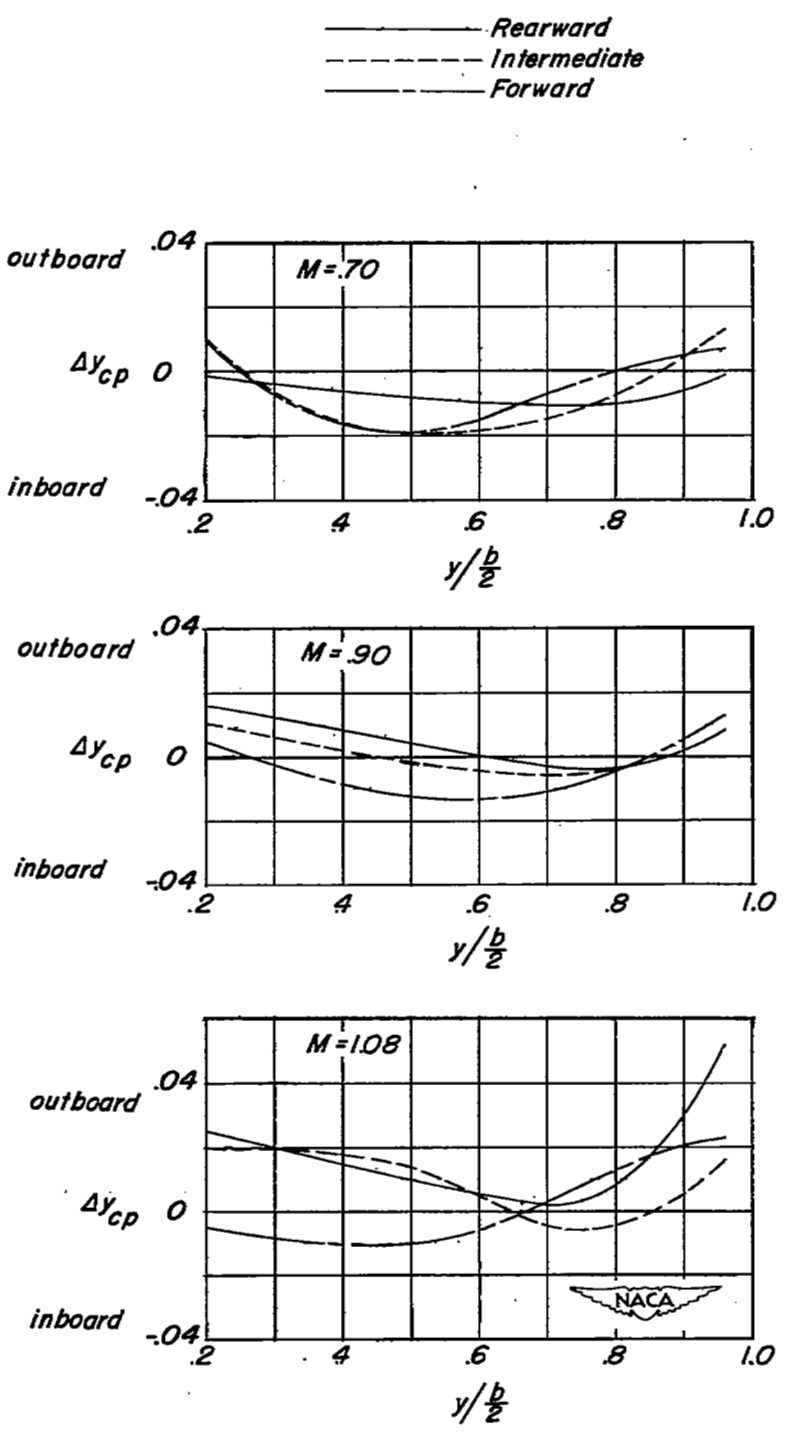

Figure 20.- Variation of the increments in lateral center-of-pressure locations with nacelle spanwise location as obtained from figure 19.

NACA-Langley - 12-18-52 - 350